Republic of Yemen
Ministry of Agriculture and Irrigation

Groundwater & Soil Conservation Project
IDA Credit 3860-YEM

Interim report

Satellite Imagery follow-up study
(RFP No. GSCP/SATELLITE IMAGERY/CQS/1/2010)
By

Remote Sensing Services
Wageningen, the Netherlands
www.waterwatch.nl

And

Hydro-Yemen

9 March 2012

Contract nr: GSCP/SATELLITE IMAGERY/CQS/1/2010

Interim report, March 2012

The authors are:

WaterWatch: Susan van der Salm, Wim Bastiaanssen and Maurits Voogt

Please send inquiries and comments to info@waterwatch.nl

All rights reserved, March 2012

Table of contents

1. Introduction

The Satellite Imagery follow-up study is executed under contract number GSCP/SATELLITE IMAGERY/CQS/1/2010. The main contractor of the project is WaterWatch, a scientific advisory bureau based in Wageningen, the Netherlands. WaterWatch specialises in remote sensing applications for agricultural water management. The sub-contractor to this project is Hydro-Yemen, an advisory firm specialised in water management, based in Sana'a, Yemen.
This study is a follow up of the 2006 project *Satellite imagery for cropping pattern and irrigated area monitoring*. Both the original project and this follow-up study aim to assist in monitoring the progress and performance of the Groundwater and Soil Conservation Project (GSCP). The objective of the GSCP is to conserve irrigation water, especially groundwater, and soils through: (i) adoption of water saving technologies; (ii) rehabilitation of terraces, small and medium sized spate irrigation schemes, bank protection works and soil conservation works; and (iii) capacity building within government institutions and community groups. The GSCP is a country wide program with the project coordination unit based in Sana'a.

Earth observation techniques can help to monitor if irrigation beneficiaries comply with legal requirements such as (i) restrictions on expansion of irrigated cropped areas after subsidised improvements of irrigation schemes and (ii) restrictions on qat production on farms provided with these improved technologies under the project. The GSCP aims to reduce crop water use, with a special focus on reducing irrigation with groundwater.

The original study established a baseline for 2006 in four study areas. Those areas were selected after discussions with members of the Groundwater and Soil Conservation Project, the National Water Resources Authority and the Central Water Management Unit of the Ministry of Agriculture and Irrigation. The study areas are all located in the west of Yemen. Study area Siham is located at the Red Sea coast in the Tihama plain; study areas Dhamar and Rada are located in the mountains of the Wadi Adhana catchment and study area Abyan is located at the coast of the Gulf of Aden.

This follow-up study aims to identify changes in land use and water consumption between 2006 and 2010. For that reason much of the methodology of the 2006 study (WaterWatch, 2009) is again used to study the land use and water consumption in 2010. This interim report presents the initial findings with regard to precipitation and temperature in the year 2010 as well as results of the fieldwork in the study areas and a trend analysis for precipitation since 1998. Also included in this interim report is a description of the study areas, of the available materials and of the methodologies used. The study of water consumption, detailed land use and comparisons between 2006 and 2010 is ongoing and those results will be included in the final report.

2. Materials

The main data source for this project is satellite imagery. This chapter gives an overview of the different types of satellite imagery used. A listing of the acquisition dates of the imagery is given as well.
The Areas of Interest of the study of 2006 were chosen based on the extent of the Spot images that were used for that study. For this 2010 study the areas are kept the same to be able to compare both years; the locations are shown in Figure 1.

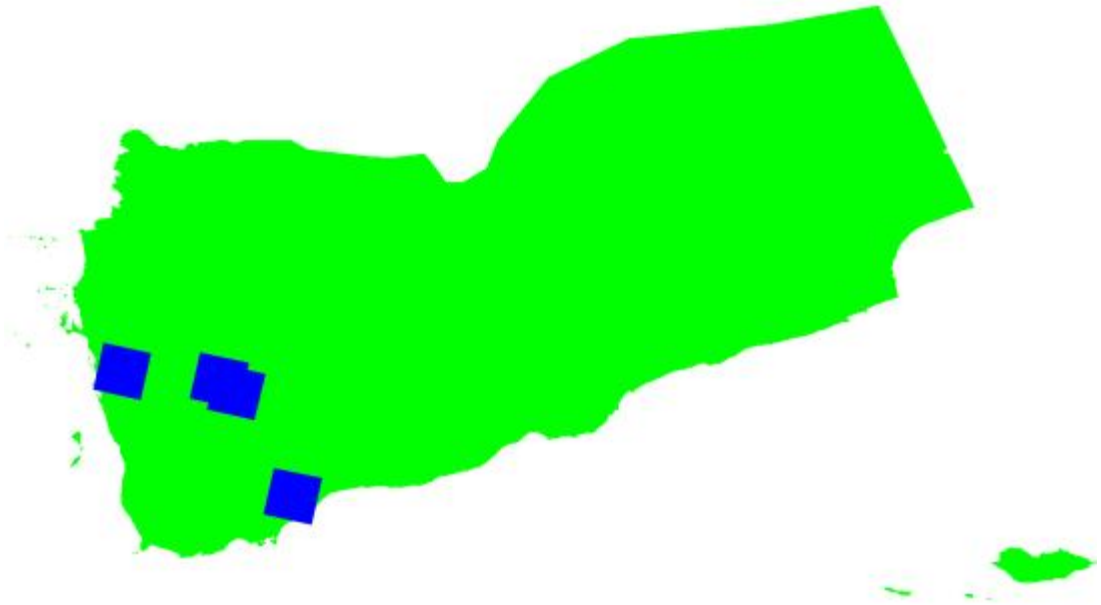

Figure 1: Areas of Interest for the study areas.

2.1 Alos images

The Alos satellite provides imagery of Yemen with a higher resolution than other satellites images that are available for 2010. For every area at least on two dates a clear image is available with Siham having been measured even on ten dates.
The ALOS satellite was launched by the Japanese Aerospace Exploration Agency in 2006 and functioned until 2011. The AVNIR-2 sensor (Advanced Visible and Near Infrared Radiometer type 2) had a resolution of 10 meters at nadir and was used to observe land cover. The characteristics of Alos are summarised in Table 1.

Table 1: Alos characteristics

Sensor	Electromagnetic Spectrum	Pixel size	Spectral bands
AVNIR-2	B1: blue	10 m	0.42 – 0.50 µm
	B2: green	10 m	0.52 – 0.60 µm
	B3: red	10 m	0.61 – 0.69 µm
	B4: near infrared	10 m	0.76 – 0.89 µm

The high resolution of the Alos images makes them very suitable to use as a basis for the land use classification as well as to downscale Modis images. The images used for this research are listed in Table 2.

Table 2: Alos acquisitions

Area	Date	Path/row	Conditions	Comments
Abyan	2010/03/25	234/3330	Clear	Northern part
Abyan	2010/03/25	234/3340	Clear	Southern part
Abyan	2010/06/25	234/3340	Clear	Shifted
Dhamar	2009/10/26	236/3300	Clear	Northern part
Dhamar	2009/10/26	236/3310	Clear	Southern part
Dhamar	2010/06/13	236/3300	Clouded	Northern part
Dhamar	2010/06/13	236/3310	Clouded	Southern part
Dhamar	2010/12/14	236/3310	Clear	Shifted
Rada	2010/04/11	235/3310	Clear	
Rada	2010/05/27	235/3310	Clear	
Rada	2010/07/12	235/3310	Clear	
Siham	2010/01/06	238/3300	Clear	North-East
Siham	2010/01/06	238/3310	Clear	South-East
Siham	2010/01/14	238/3310	Clear	South-East
Siham	2010/01/31	239/3300	Clear	West
Siham	2010/02/12	238/3310	Clear	South-East
Siham	2010/03/18	239/3300	Clear	West
Siham	2010/04/16	238/3300	Few clouds	North-East
Siham	2010/04/16	238/3310	Few clouds	South-East
Siham	2010/06/18	239/3300	Few clouds	West
Siham	2010/10/17	238/3310	Few clouds	South-East
Siham	2010/11/03	239/3300	Clear	West
Siham	2010/12/19	239/3300	Clear	West

From this table it can be seen that the Siham area is included in three Alos frames (238/3300 North-East; 238/3310 South-East and 239/3300 West). This means that per frame only a part of the study area is shown (as can be seen in the quick look overviews in Figure 6 of Chapter 3).

2.2 Aster images

Another satellite sensor that provides images with a good resolution is ASTER (Advanced Space borne Thermal Emission and Reflection radiometer). This Japanese sensor is onboard of the NASA satellite Terra. Its resolution is 15 meters for the visible light and near infrared; 30 meters for the short-wave infrared measurements and 90 meters for measurements in the thermal infrared part of the electromagnetic spectrum. The characteristics of the Aster sensor are listed in Table 3.

Table 3: Aster characteristics

Electromagnetic Spectrum	Pixel size	Spectral bands
B1: green/yellow	15 m	0.52 – 0.60 µm
B2: red	15 m	0.63 – 0.69 µm
B3: near infrared nadir	15 m	0.76 – 0.86 µm
B4: near infrared backward	15 m	0.76 – 0.86 µm
B5: short-wave infrared	30 m	1.60 – 1.70 µm
B6: short-wave infrared	30 m	2.145 – 2.185 µm
B7: short-wave infrared	30 m	2.185 – 2.225 µm
B8: short-wave infrared	30 m	2.235 – 2.285 µm
B9: short-wave infrared	30 m	2.295 – 2.365 µm
B10: short-wave infrared	30 m	2.360 – 2.430 µm
B11: thermal infrared	90 m	8.125 – 8.475 µm
B12: thermal infrared	90 m	8.475 – 8.825 µm
B13: thermal infrared	90 m	8.925 – 9.275 µm
B14: thermal infrared	90 m	10.25 – 10.95 µm
B15: thermal infrared	90 m	10.95 – 11.65 µm

Only four images from the archive show the study areas. These four dates are listed in Table 4. The images for Dhamar and Rada add to the Alos images to cover enough moments throughout the year to be able to classify the land use in those areas.

Table 4: Aster acquisitions

Area	Date	Conditions	Comments
Dhamar and Rada	2010/06/26	Clear	
Rada	2009/10/22	Clear	
Siham	2010/02/18	Few Clouds	North
Siham	2010/12/03	Clear	South

2.3 Landsat images

Another satellite program from which images are used in this project is the Landsat Program. Landsat 5 was already launched in 1984 and, among other sensors, it carries the Thematic Mapper that takes multi-spectral images. Although Landsat 5 was still working, Landsat 6 was launched in 1993. The new satellite was equipped with an added panchromatic band to enhance the Thematic Mapper but it failed to reach orbit and therefore hasn't been operational. After six years, in 1999 Landsat 7 was launched. It is the latest satellite of the Landsat Program to date. The sensor onboard Landsat 7 is the Enhanced Thematic Mapper (ETM), with a panchromatic band added to the original Thematic Mapper and an improved resolution on the thermal band.
Since May 31, 2003 the Landsat 7 ETM sensor did not function properly. The scan line corrector failed and has not been repaired since. The result of this failure is that some areas are imaged twice and some not at all. The effect is visible in the images as a set of missing lines increasing in width from the middle of the image to the border of the images. A net effect is that approximately 25% of an image is missing. To solve this problem the images are gap-filled with data from other satellites from that same time and with older data from the Landsat satellites. Table 5 gives an overview of the main characteristics of the Landsat sensors (Thematic Mapper on Landsat 5 and Enhanced Thematic Mapper on Landsat 7).

Table 5: Landsat 5 and 7 characteristics

Sensor	Electromagnetic Spectrum	Pixel size	Spectral bands
Landsat 5: TM	B1: blue	30 m	0.45 – 0.52 µm
	B2: green	30 m	0.52 – 0.60 µm
	B3: red	30 m	0.63 – 0.69 µm
	B4: near infrared	30 m	0.76 – 0.90 µm
	B5: shortwave infrared	30 m	1.55 – 1.75 µm
	B6: thermal infrared	120 m	10.4 – 12.5 µm
	B7: shortwave infrared	30 m	2.08 – 2.35 µm
Landsat 7: ETM	Panchromatic	15 m	0.50 – 0.90 µm
	B1: blue	30 m	0.45 – 0.52 µm
	B2: green	30 m	0.52 – 0.60 µm
	B3: red	30 m	0.63 – 0.69 µm
	B4: near infrared	30 m	0.75 – 0.90 µm
	B5: shortwave infrared	30 m	1.55 – 1.75 µm
	B6: thermal infrared	60 m	10.4 – 12.5 µm
	B7: shortwave infrared	30 m	2.08 – 2.35 µm

Table 6 gives an overview of the Landsat data used in this study. For the first part of the measuring period also Landsat 5 images are available. The advantage of these images is that they are complete, without gaps.
Despite the somewhat courser resolution, this set of images has been of great help to describe the dynamic changes of local scale processes such as cropping patterns and land use. The Landsat 7 data have been patched using either concurrent satellite images or historical Landsat data.

Table 6: Landsat 5 and 7 acquisitions

Area	Date	Path/row	Conditions	Comments
Abyan	2009/10/22	165/51	Clouded	Landsat 7 - need to be gap filled
Abyan	2009/12/17	165/51	Clouded	Landsat 5
Abyan	2010/01/18	165/51	Clouded	Landsat 5
Abyan	2010/03/15	165/51	Clear	Landsat 7 - need to be gap filled
Abyan	2010/10/09	165/51	Clear	Landsat 7 - need to be gap filled
Abyan	2010/10/25	165/51	Clouded	Landsat 7 - need to be gap filled
Dhamar	2009/11/22	166/50	Clear	Landsat 5
Dhamar	2009/12/08	166/50	Clear	Landsat 5
Dhamar	2010/02/10	166/50	Clear	Landsat 5
Dhamar	2010/04/07	166/50	Clear	Landsat 7 - need to be gap filled
Dhamar	2010/04/23	166/50	Clear	Landsat 7 - need to be gap filled
Dhamar	2010/09/14	166/50	Few clouds	Landsat 7 - need to be gap filled
Dhamar	2010/09/30	166/50	Clear	Landsat 7 - need to be gap filled
Dhamar	2010/10/16	166/50	Clear	Landsat 7 - need to be gap filled
Rada	2010/01/18	165/50	Clear	Landsat 5
Rada	2010/01/26	165/50	Clear	Landsat 7 - need to be gap filled
Rada	2010/03/15	165/50	Clear	Landsat 7 - need to be gap filled
Rada	2010/09/23	165/50	Clear	Landsat 7 - need to be gap filled
Rada	2010/10/09	165/50	Clear	Landsat 7 - need to be gap filled
Rada	2010/10/25	165/50	Clear	Landsat 7 - need to be gap filled
Siham	2009/11/22	166/50	Few clouds	Landsat 5
Siham	2009/12/08	166/50	Few clouds	Landsat 5
Siham	2010/02/10	166/50	Clouded	Landsat 5
Siham	2010/04/07	166/50	Clear	Landsat 7 - need to be gap filled
Siham	2010/04/23	166/50	Few clouds	Landsat 7 - need to be gap filled
Siham	2010/09/14	166/50	Clouded	Landsat 7 - need to be gap filled
Siham	2010/09/30	166/50	Clouded	Landsat 7 - need to be gap filled
Siham	2010/10/16	166/50	Clear	Landsat 7 - need to be gap filled

2.4 Modis images

There is a Modis sensor (Moderate-resolution Imaging Spectroradiometer) located onboard the Aqua and one onboard the Terra satellite. Both satellites were launched by NASA. They cover the whole world in one day. It is therefore possible to have two Modis images for the same area for one day. The difference between the two platforms lies in the overpass time. Terra has an overpass time before noon, whereas Aqua has an overpass time in the afternoon. Modis has a swath width of 2330 km, making it very useful to gather data for large areas.

The Modis sensor has two bands with a resolution of 250 meters, the red and near infrared. It is therefore possible to obtain the Normalized Difference Vegetation Index (NDVI) at a resolution of 250 meters. The Modis sensor also has five bands in the visible and near infrared region of the electromagnetic spectrum. These bands have a resolution of 500 meters. The Modis sensor further has a large number of bands in the thermal infrared spectrum. Two of those, at 11 and 12 micrometers, can be used to calculate the surface temperature. These data have a resolution of 1000 meters. The characteristics of the Modis sensor are summarised in Table 7.

Table 7: Modis characteristics

Electromagnetic Spectrum	Pixel size	Spectral bands
B1: red	250 m	0.62 – 0.67 µm
B2: near infrared	250 m	0.84 – 0.87 µm
B3: blue	500 m	0.46 – 0.48 µm
B4: green	500 m	0.54 – 0.56 µm
B5: shortwave infrared	500 m	1.23 – 1.25 µm
B6: shortwave infrared	500 m	1.62 – 1.65 µm
B7: shortwave infrared	500 m	2.10 – 2.15 µm
B31: thermal infrared	1000 m	10.78 – 11.28 µm
B32: thermal infrared	1000 m	11.77 – 12.27 µm

With the aid of these Modis data calculations of the energy balance algorithm are carried out for the western part of Yemen for the year 2010. The energy balance algorithm is explained in paragraph “3.1 Water consumption”. A list of the Modis data used in the calculations is given in Table 8.

For these calculations composite images are used instead of single images. These composite images are created by NASA from satellite images of a period of 16 days. The images are combined to minimise cloud cover in the resulting composite. Due to the combining of images of sixteen days, Modis images are available for every period of the year.

Table 8: Modis acquisitions

Period	Starting date	End date
1	2009/12/27	2010/01/08
2	2010/01/09	2010/01/24
3	2010/01/25	2010/02/09
4	2010/02/10	2010/02/25
5	2010/02/26	2010/03/13
6	2010/03/14	2010/03/29
7	2010/03/30	2010/04/14
8	2010/04/15	2010/04/30
9	2010/05/01	2010/05/16
10	2010/05/17	2010/06/01
11	2010/06/02	2010/06/17
12	2010/06/18	2010/07/03
13	2010/07/04	2010/07/19
14	2010/07/20	2010/08/04
15	2010/08/05	2010/08/20
16	2010/08/21	2010/09/05
17	2010/09/06	2010/09/21
18	2010/09/22	2010/10/07
19	2010/10/08	2010/10/23
20	2010/10/24	2010/11/08
21	2010/11/09	2010/11/24
22	2010/11/25	2010/12/10
23	2010/12/11	2010/12/26
24	2010/12/27	2011/01/8

3. Methodology

The satellite images are combined with other data such as meteorological measurements and data from fieldwork. To identify the agricultural land use and the water consumption of the four study areas in Yemen, these inputs have to be processed by techniques. These techniques are explained in this chapter.
The land use is identified based on satellite images, because different land use types reflect and absorb radiation in different ways, not only the visible light, but also the infrared radiation and the thermal radiation.
The water consumption is mapped with a surface energy balance algorithm for land surfaces, which was developed by Bastiaanssen. These algorithms not only use satellite data, but also use meteorological observations of ground stations. It may seem strange to use an energy balance to calculate water consumption, but the energy balance and the water balance are actually coupled. Evapotranspiration is not only a loss term in the water balance, but also in the energy balance, because it requires energy to evaporate water. Measuring the energy balance from satellite imagery provides pixel based information on water consumption. Measuring the water balance requires elaborate and costly measurements in the field and can only be done on catchment scale; a much coarser spatial pattern would be the result.

3.1 Water consumption

Energy balance algorithms not only compute evapotranspiration (potential and actual), but can also map biomass growth and soil moisture content. In this current project the focus is to compute potential and actual evapotranspiration (ET). The potential evapo-transpiration (ET_{pot}) is the amount of water that could evaporate from the soil and transpire from the plant in case the area is well-watered, under the actual meteorological conditions and the present vegetation. Well-watered and healthy plants can grow optimally and they will produce the potential yield. When, however, there is not enough water available to the plants, they stop transpiration to save water. To stop the loss of water, the stomata close and the uptake of CO_2 will stop, this will result in a lower actual evapotranspiration (ET_{act}). CO_2 is an important contribution to biomass, so a decreased uptake of CO_2 limits the plants growth and the resulting yield will be lower.

The surface energy balance algorithm for land surfaces used in this study is an image processing tool that calculates actual and potential evapotranspiration rates as well as other energy exchanges between the land surface and the atmosphere. The satellite images that are processed by this tool consist of raster values of spectral radiance in the visible, near-infrared and thermal infrared part of the electromagnetic spectrum. Since these radiances vary between pixels, every pixel is calculated individually. However, the energy balance algorithm also requires some ground-measured meteorological parameters to calculate potential evapotranspiration. The required weather data parameters are:

- Wind speed
- Humidity
- Solar radiation
- Air temperature

To calculate ET, both potential and actual, meteorological parameters alone are not sufficient. To be able to estimate the evapotranspiration not only for the location of the weather station, but for the whole study area, more spatial data has to be used. Land surface characteristics such as surface albedo (reflection coefficient), leaf area index, vegetation index and surface temperature can be converted from the satellite radiances. Digital elevation models and land use maps are used to determine the surface roughness, which affects the interactions between the land surface and the atmosphere, such as ET_{act}.

A more elaborate and technical description of the Surface Energy Balance Algorithm for Land (SEBAL) can be found in Appendix 1.

3.2 Fieldwork

Fieldwork is required to improve and validate the satellite based land use classification, which will be presented in the final report. The fieldwork for this project is carried out by Hydro-Yemen in the study areas Siham, Dhamar and Rada. Equipped with a GPS-transponder fields were visited across the study areas to describe crop type and irrigation type. In Figure 2 an example is given of where the field information is collected. Six crop types are distinguished:

- Rainfed
- Single-season, irrigated
- Double-season, irrigated
- Perennial
- Banana
- Qat

And also six classes are distinguished for irrigation type:

- Border
- Furrow
- Drip
- Improve irrigation
- Sprinkler
- Bubbler

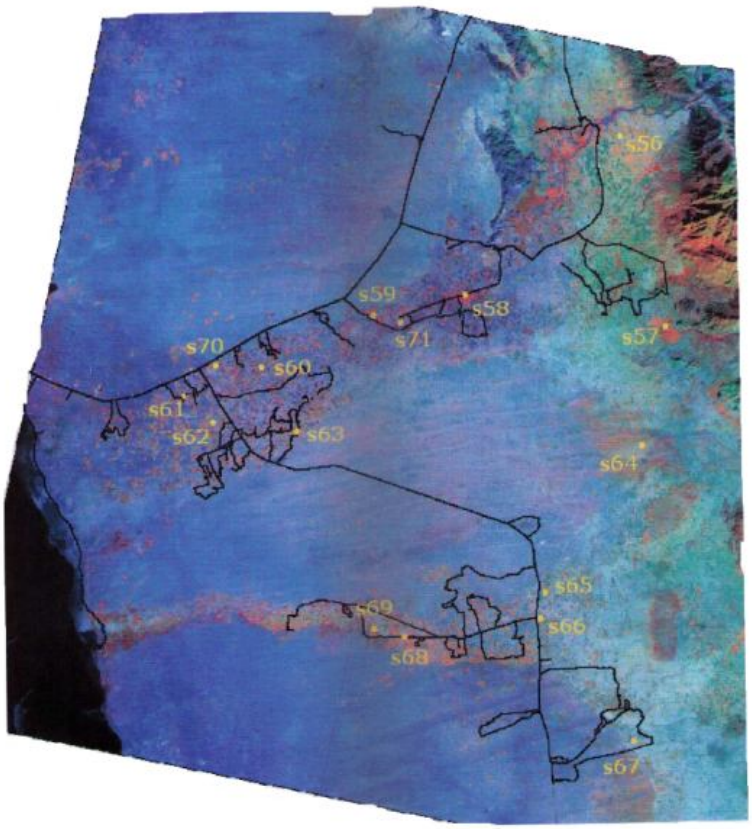

Figure 2: Overview of fieldwork locations in the Siham study area with in yellow field site locations and in black the GPS-track.

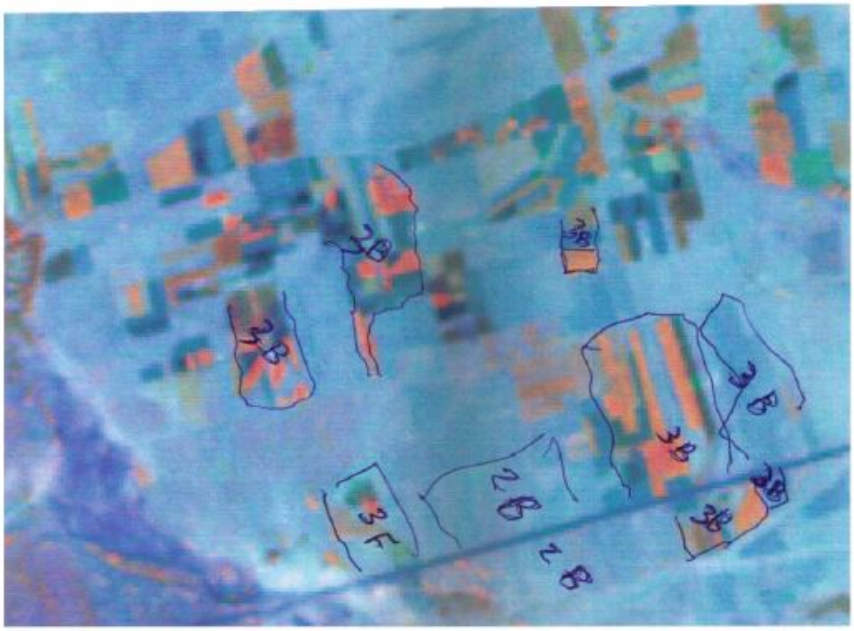

Figure 3: Example of field notes from location s67, located in the South of the Siham area.
2 = Single-season irrigated crop; B = Border irrigated;
3 = Double-season irrigated crop; F = Furrow irrigated

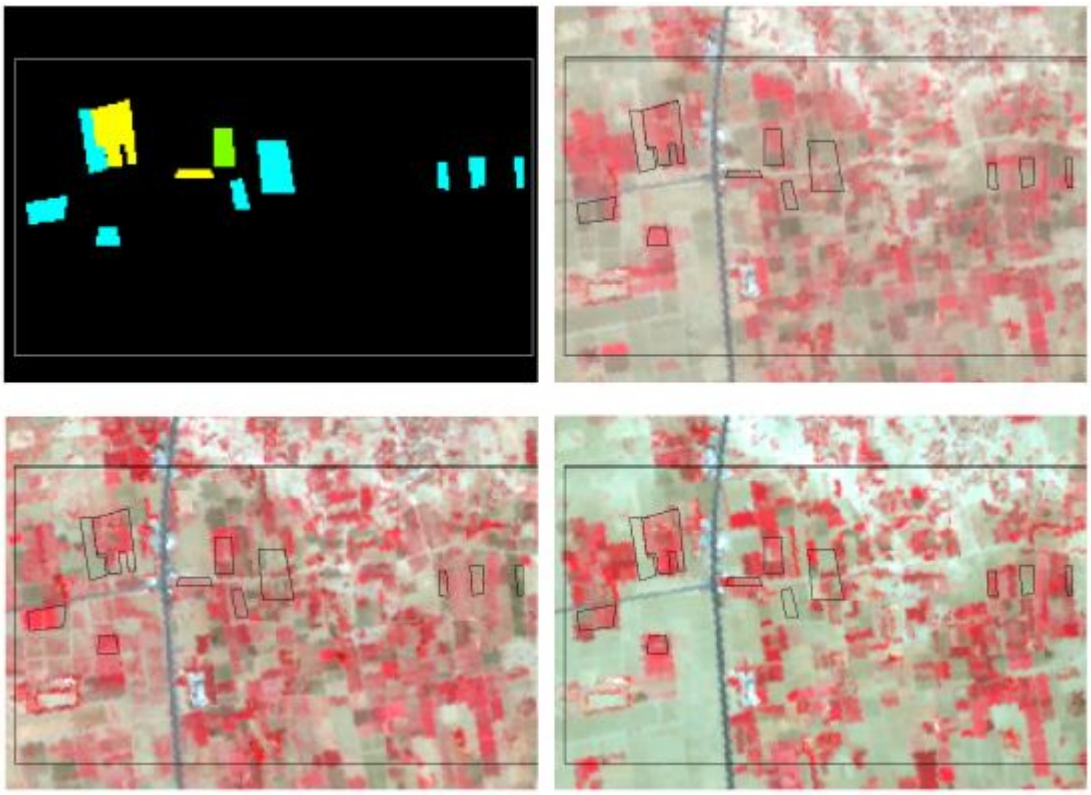

Figure 4: Digitalisation of the field work, site s66 in the Siham study area. Upper left corner: crop class: yellow is perennial; green is double season irrigated and turquoise blue is single season irrigated. The other panels are Alos satellite images with the shape of the fields overlain. The acquisition dates of the Alos images are: Upper right corner: 14 January 2010; Lower left corner: 12 February 2010 and Lower right corner: 16 April 2010.

In Figure 4 an example is shown of how the fieldwork is digitised. This site in the Siham study area is irrigated by border irrigation and the main crop type is single-season irrigated crops. From this figure it can be seen that there is not a specific growing season. Some single-season fields are most productive in February (like the marked field most to the left) while other fields are more productive in April (for example the 3rd marked field from the right). Other fields are not productive in the images shown or are productive in all images. The yellow (perennial) and green (double-season) fields from the upper right panel are productive (red-coloured) in all of the three images shown here, so to distinguish between those more images are used.

4. Siham

4.1 General

Of the four study areas, Siham is the western area, more or less half-way along the western coast line.

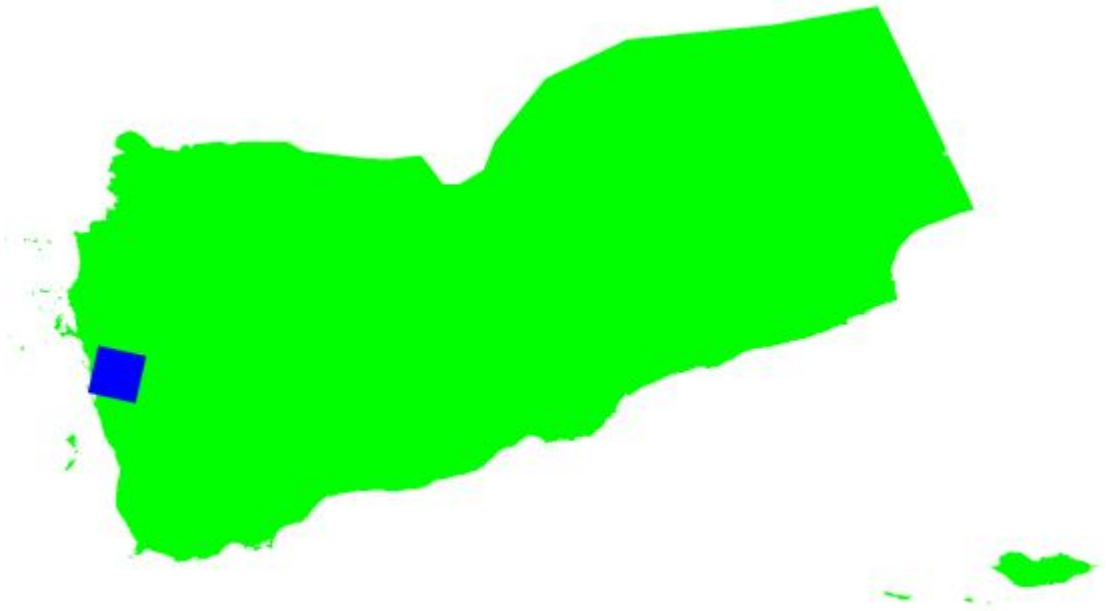

Figure 5: The Area of Interest of the Siham study area.

The Siham study area consists of two wadis and the plain area in between. These wadis lie in the Tihama plain in the West of Yemen, at the Red Sea Coast. The Northern wadi is called Wadi Siham and the Southern wadi is called Wadi Jahbah.

For Siham many satellite images are available: for 10 dates there are images from Alos; 2 from Aster and 8 from Landsat. These 20 dates are spread over the year, but with only one image in the May – August period. The images made by Alos are shown in Figure 6. In these images, the blue framework represents the study area as defined in the 2006 study. Since the new images are recorded by other satellites, the area covered does not exactly match the Area of Interest. This makes it a bit more difficult to have a good overview of changes throughout the year.

The images are displayed in so-called False Colour composite. This means that instead of displaying the bands blue, green and red (which would result in normal colours), the bands green, red and near-infrared are displayed. High measurements in the near-infrared part of the spectrum are shown as bright red in the images; these red areas mainly contain growing plants. In this way ‘bright red’ implies that the plants have water, for the dry season it means that the fields are irrigated. The main system of irrigation in the wadis of the Siham study area is spate irrigation.

Something else that can be seen from these images is that the mountainous area, in the south-east of the blue framework, has most vegetation in October. This is clearest when comparing 17 October 2010 to 1 June 2010. The dark blue – black colours show the sea, which absorbs most radiation and hardly reflects in the wavelengths shown here.

White areas are caused by high reflection in all bands. This can be bare soil but it could also be caused by clouds.

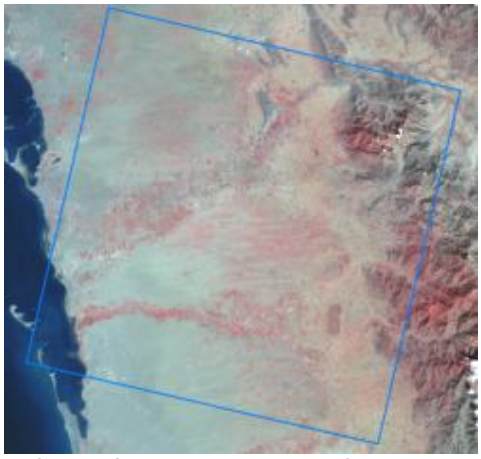

a) Landsat 7 - 22 November 2009

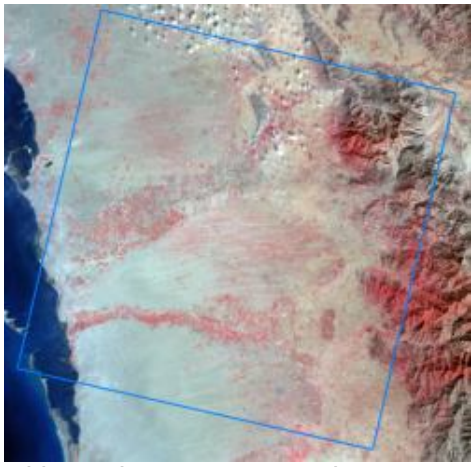

b) Landsat 5 - 8 December 2009

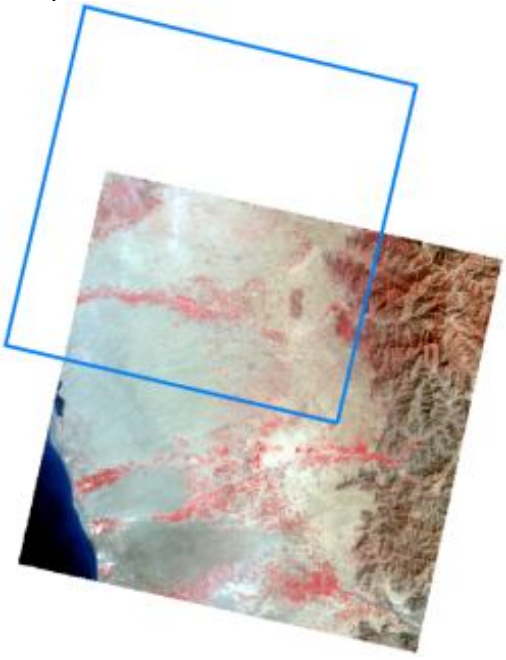

c) Alos - 14 January 2010

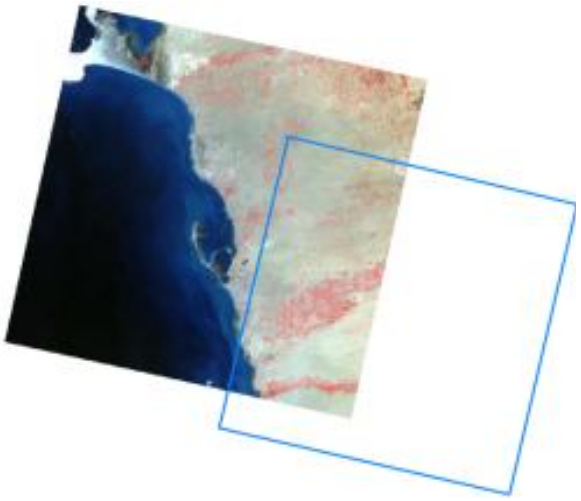

d) Alos - 31 January 2010

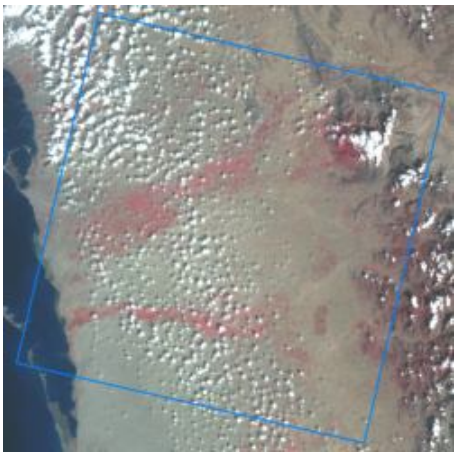

e) Landsat 5 - 10 February 2010

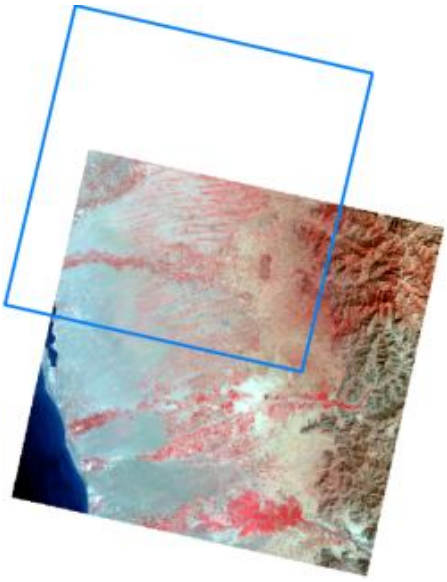

f) Alos - 12 February 2010

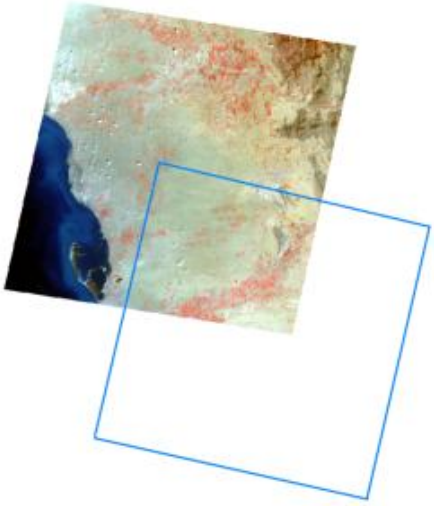

g) Aster - 18 February 2010

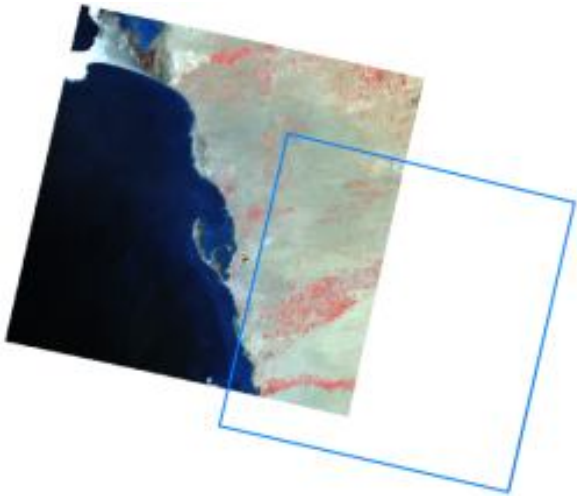

h) Alos - 18 March 2010

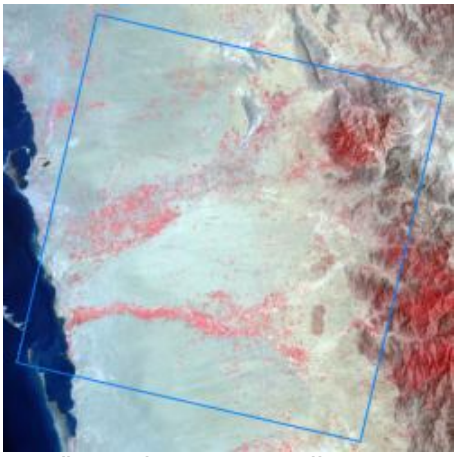

i) Landsat 7 - 7 April 2010

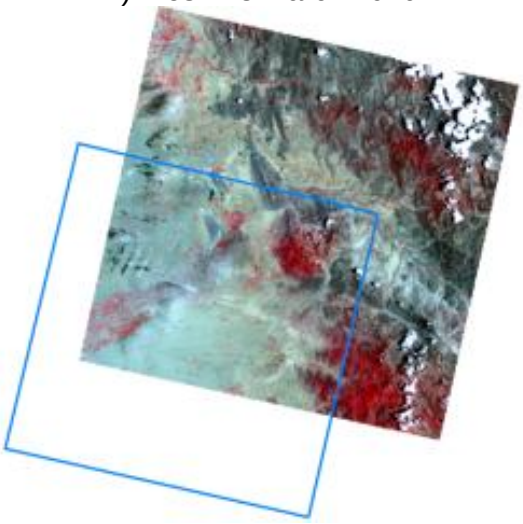

j) Alos - 16 April 2010

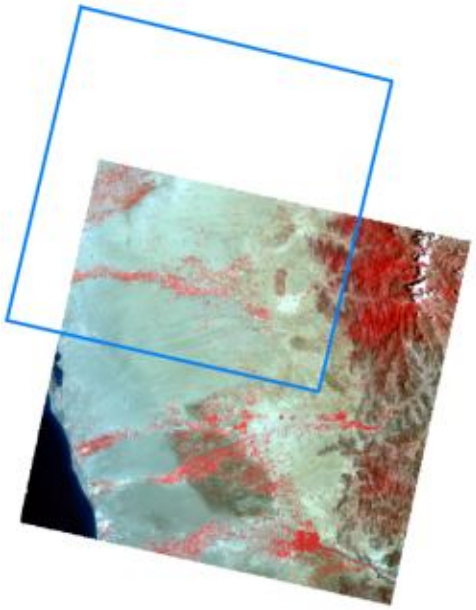

k Alos - 16 April 2010

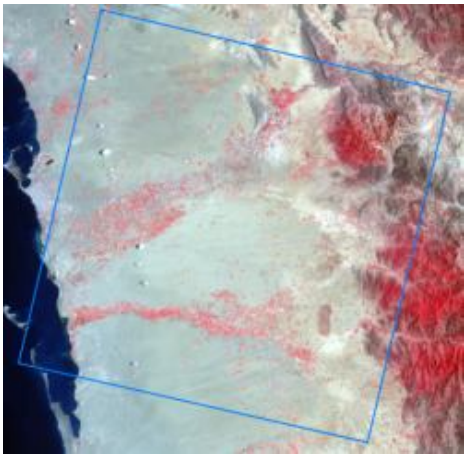

l) Landsat 7 - 23 April 2010

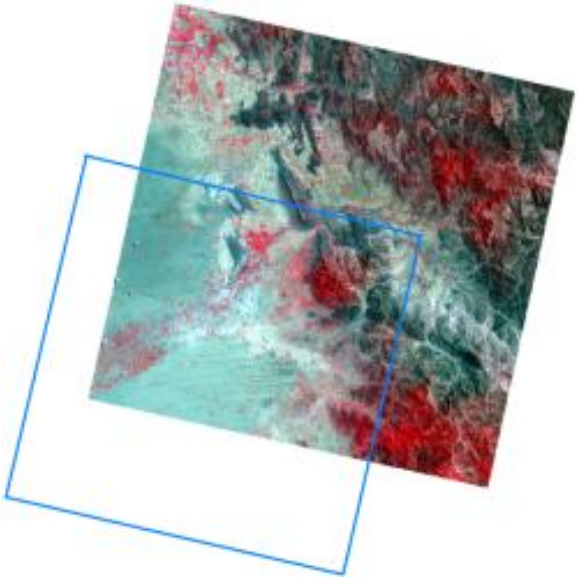

m) Alos - 1 June 2010

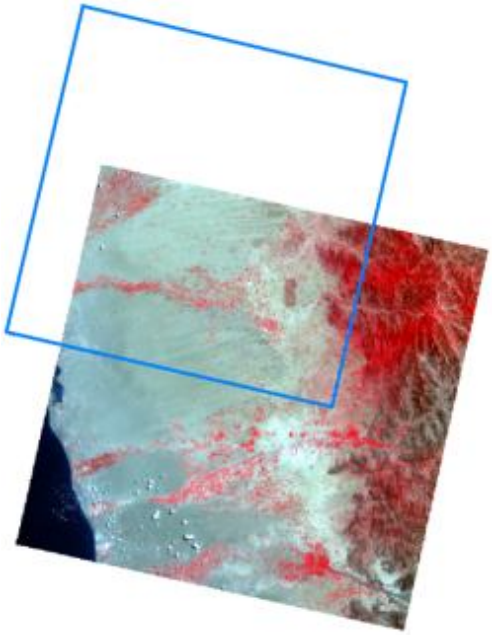

n) Alos - 1 June 2010

o) Alos - 18 June 2010

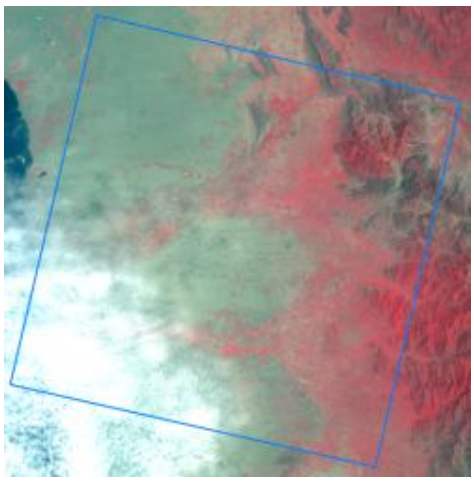

p) Landsat 7 - 14 September 2010

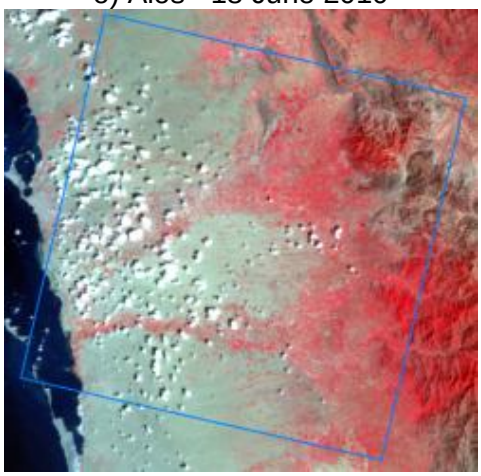

q) Landsat 7 - 30 September 2010

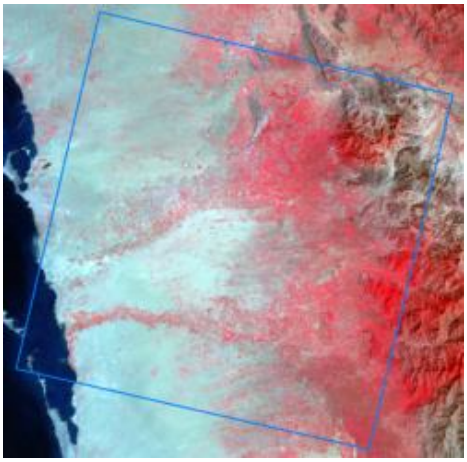

r) Landsat 7 - 16 October 2010

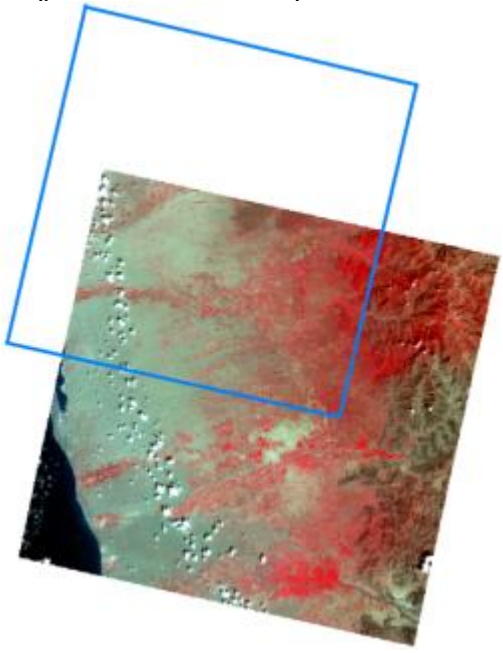

s) Alos - 17 October 2010

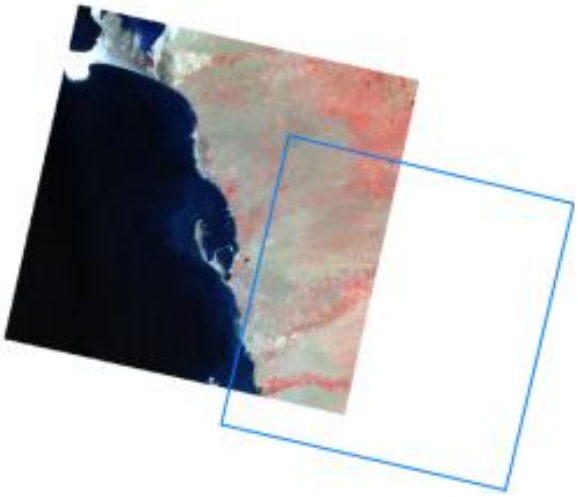

t) Alos - 3 November 2010

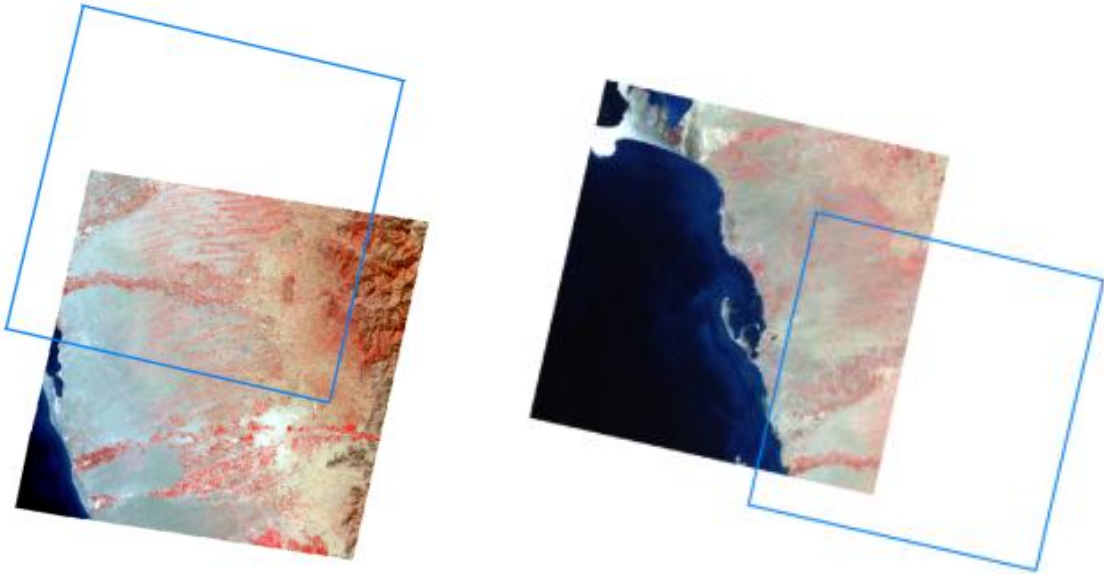

u) Aster - 3 December 2010 v) Alos - 19 December 2010

Figure 6: Satellite images of the Siham study area, with in blue the extent of the study area.

4.2 Climate

Figure 7 shows the total monthly precipitation for the Siham area in 2010, based on TRMM rainfall data. The higher area in the east of the study area receives more rainfall than the coastal part of the study area. The average annual rainfall for 2010 is estimated to be 492 mm for Siham, making Siham the study area with most rain. In 2006 the amount of rain was estimated to be 519 mm. The difference between both years is that in 2010 there was rain in June but a lower peak in July and August and less rain in the end of the year.

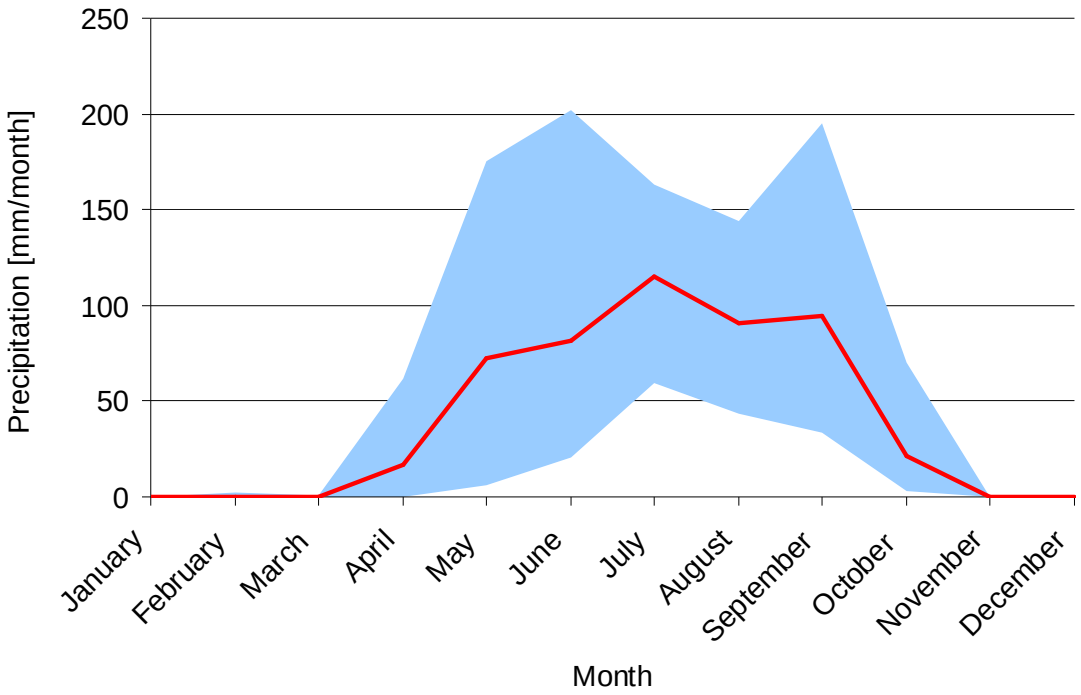

Figure 7: Monthly precipitation for the Siham area. The red solid line shows the average rainfall for the total area. The blue area shows the range of rainfall for the total area.

Figure 8: Location of Al Hudaydah meteorological station (blue dot) within the study area Siham (blue outline).

In Figure 8 the location of the meteorological station Al Hudaydah is shown. The air temperature that is measured at this location during 2010 is shown in Figure 9. There is a clear annual pattern in these measurements with temperatures in summer being approximately 10°C higher than in winter and with only small deviations from that pattern.

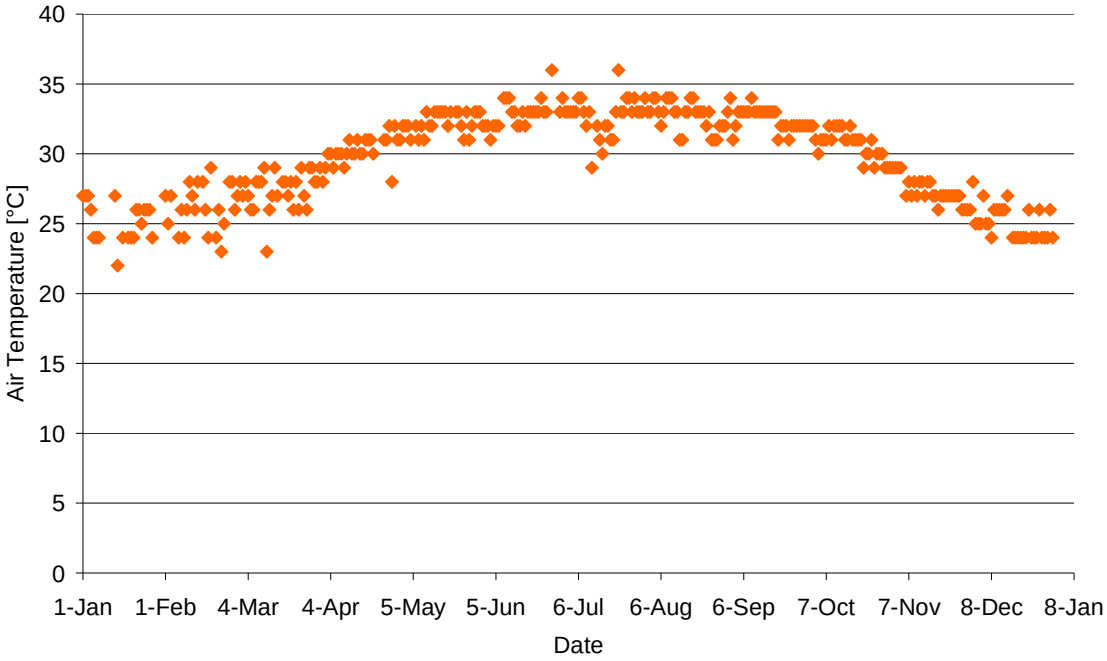

Figure 9: Daily air temperature values [°C] for the year 2010, Al Hudaydah meteorological station [Latitude 14.8° N; Longitude 43.0° E; Altitude 115 m].

The meteorological station Al Hudaydah, together with the station in Aden (for the Abyan study area), are the warmer locations with temperatures approaching 35°C, most probably due to their lower altitude. Because of these high temperatures, crops will need more water, but the higher winter temperatures also accommodate a second cropping season, under the condition that there is sufficient water available.

4.3 Fieldwork

The fieldwork is executed in the agricultural areas of the Siham study area. Almost all sites that were inspected were irrigated by border irrigation. The crop type shows a gradient from the coast to the mountains. Closer to the coast many fields have two crops; more to the east farmers grow single-season irrigated crops while in the mountains most crops are rain fed. The most notable exception is site s67 in the south of the study area: fields there have double-season irrigated agriculture.

5. Dhamar

5.1 General

Of the four study areas, Dhamar is the first highland area, approximately 50 km south of Sana'a and to the west of Rada.

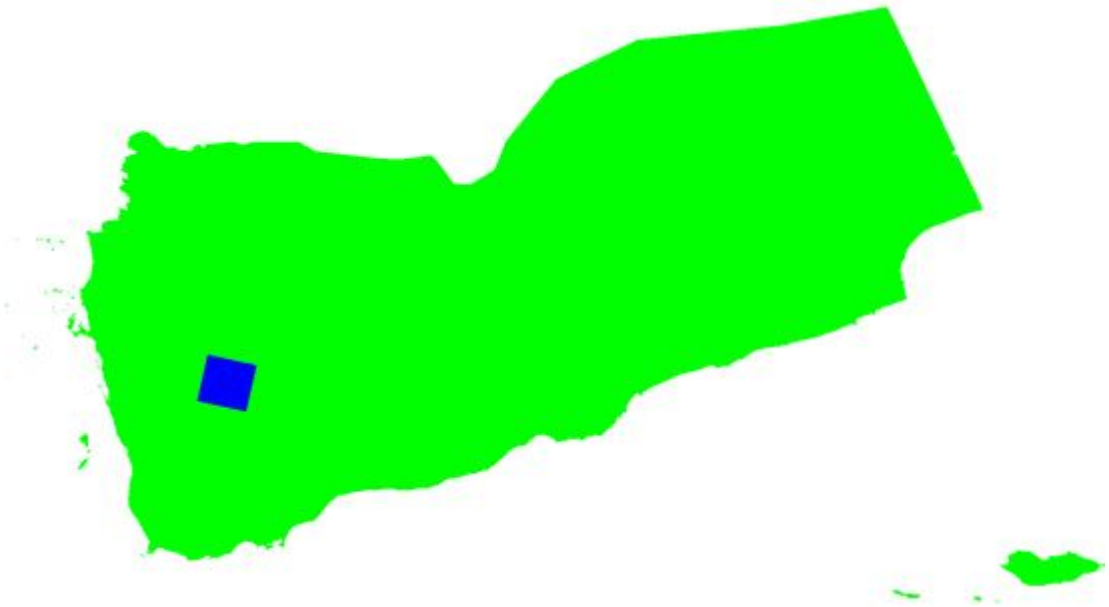

Figure 10: The Area of Interest of the Dhamar study area.

The Dhamar study area lies in the highlands of Yemen. In contrast to the coastal areas, where spate irrigation can be practiced, irrigation water in the highlands usually comes from the groundwater.
Satellite images made on 12 days show the Dhamar area: 3 images from Alos, 1 from Aster and 8 from Landsat. These 12 days are well spread over the year so that the number of crops could be determined. The images made by Alos are shown on the next page in Figure 11. The images are displayed in so-called False Colour composite. This means that instead of displaying the bands blue, green and red (which would result in normal colours), the bands green, red and near-infrared are displayed. High measurements in the near-infrared part of the spectrum are shown as bright red in the images; these red areas mainly contain growing plants. In this way 'bright red' implies that the plants have water. In the image of October more red areas are present than in December. Next to the red areas, many parts of these images are greyish, indicating none or scarce vegetation in the mountains. White areas indicate bare soil or clouds. Clouds often cast a shadow on the land surface, resulting in darker colours and a somewhat three-dimensional appearance of the clouds. Another way to distinguish between clouds and bare soil is to compare images in time: usually clouds will only occur in a few images while bare soil often is bare for longer periods.

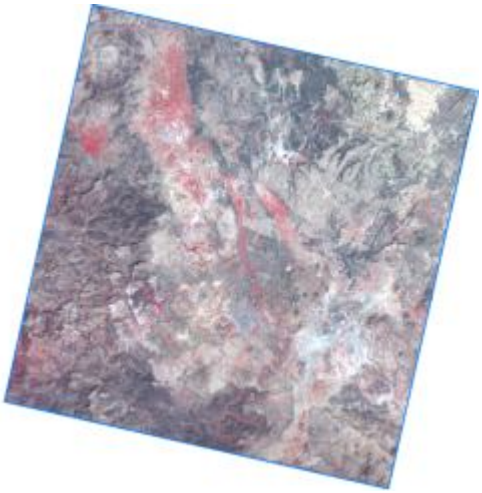

a) Alos - 26 October 2009

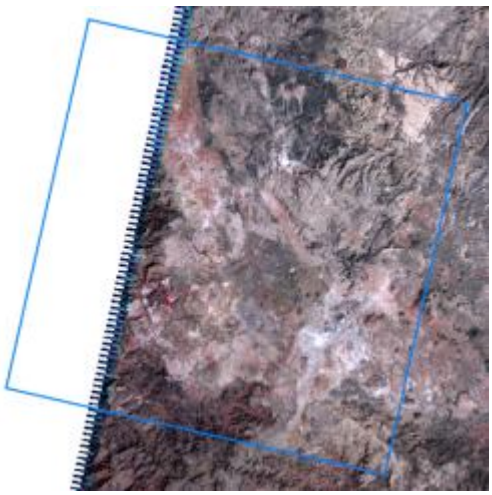

b) Landsat 5 - 18 January 2010

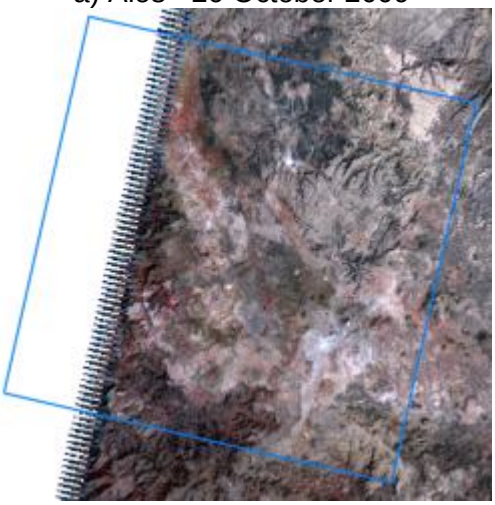

c) Landsat 7 - 26 January 2010

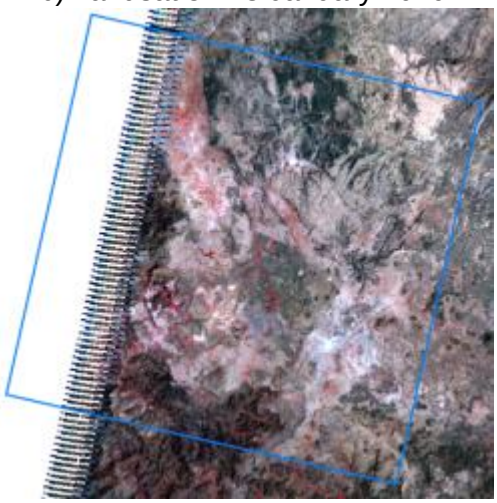

d) Landsat 7 - 15 March 2010

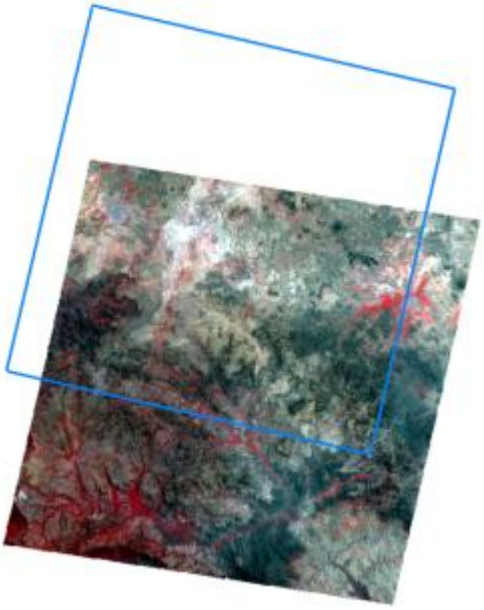

e) Aster - 26 June 2010

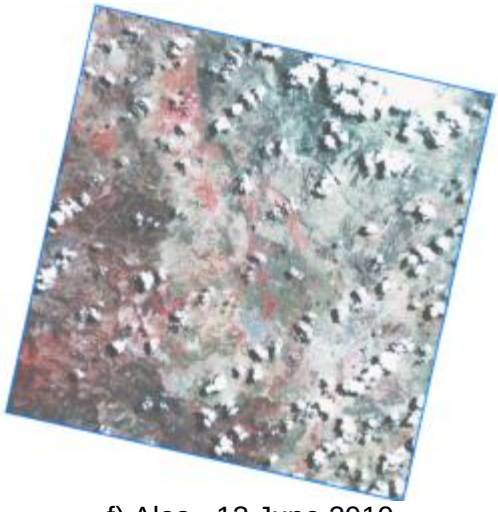

f) Alos - 13 June 2010

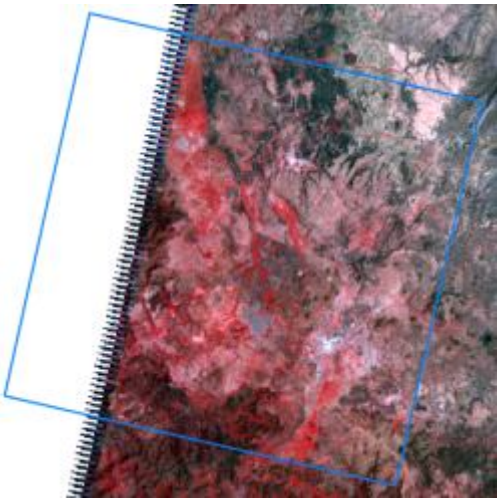

g) Landsat 7 - 23 September 2010

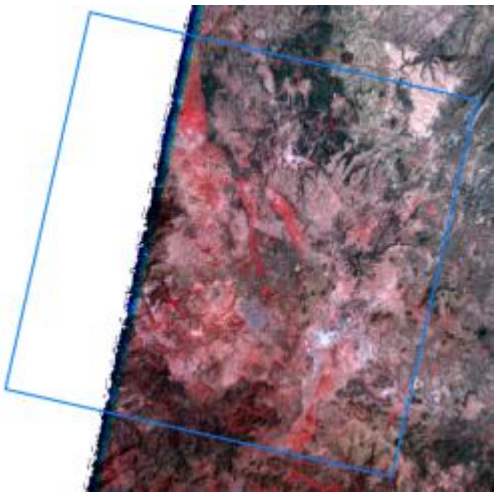

h) Landsat 7 - 09 October 2010

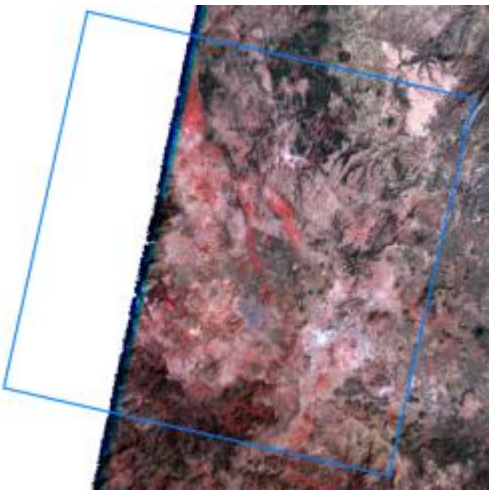

i) Landsat 7 - 25 October 2010

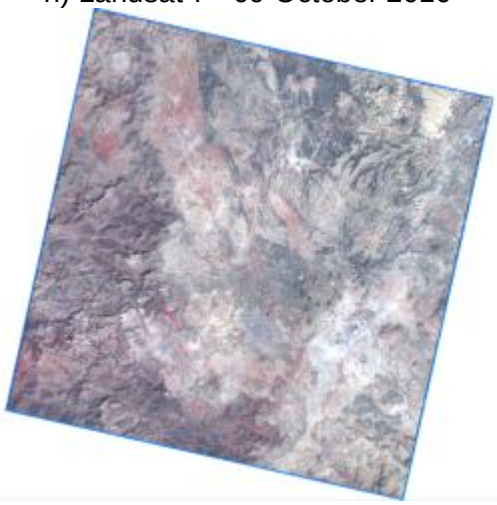

j) Alos - 14 December 2010

Figure 11: Satellite images of the Dhamar study area, with in blue the extent of the study area.

5.2 Climate

Figure 12 shows the total monthly precipitation for the Dhamar area in 2010, based on TRMM rainfall data. The south-west of the study area receives slightly more rainfall than the north-eastern part of the study area. The average annual rainfall for 2010 is estimated to be 405 mm for Dhamar. In 2006 the amount of rain is estimated to be 508 mm. The difference between both years is quite large. The first rainfall period (March, April, May) yields more rainfall in 2010 than in 2006, but the second rainfall period (July, August, September) as well as the end of the year are drier in 2010 than in 2006.

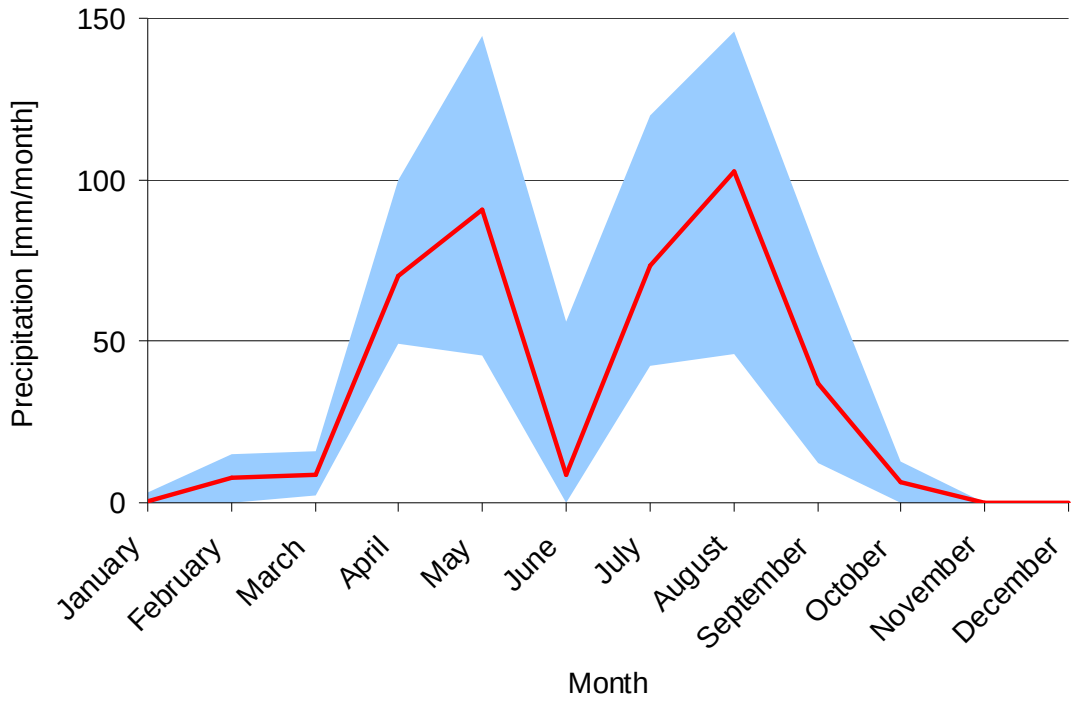

Figure 12: Monthly precipitation for the Dhamar area. The red solid line shows the average rainfall for the total area. The blue area shows the range of rainfall for the total area.

Figure 13: Location of the meteorological stations Sana'a (upper blue dot) and Dhamar (blue dot within the frame), with study area Dhamar shown in blue outline. Clearly Sana'a is located outside the study area.

Figure 13 shows the Dhamar study area, with an indication for the location of the meteorological stations of Dhamar and Sana'a. The measurements of these stations from 2010 can be seen in Figure 14.

There is an annual pattern in these measurements with temperatures in summer being approximately 10°C higher than in winter and the deviations from that pattern are larger than the ones observed in the coastal study areas.

The meteorological station Dhamar, together with the station in Sana'a, some 50 km south of Dhamar, are the cooler locations with temperatures below 25°C, due to their higher altitude of more than 2000 meters. Since the Dhamar meteorological station doesn't have records for most of February and March 2010, the meteorological station of Sana'a is shown in the graph as well.

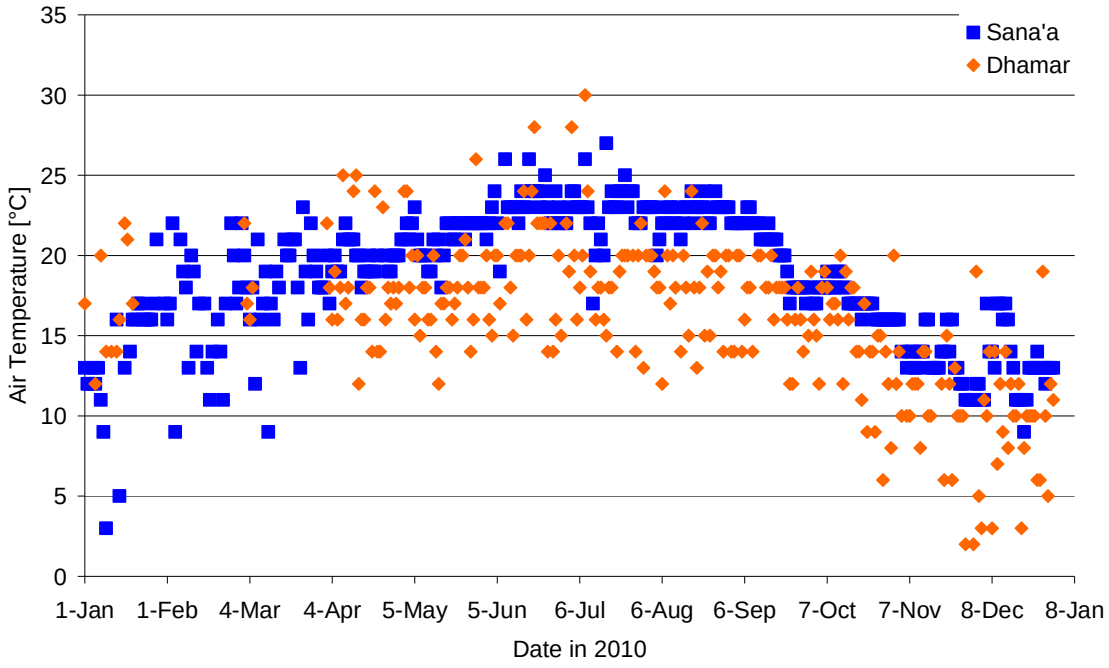

Figure 14: Daily air temperature values [°C] for the year 2010, Dhamar meteorological station [Latitude 14.6° N; Longitude 44.4° E; Altitude 2425 m]. In February and March periods are missing. Therefore also measurements from Sana'a meteorological station are shown [Latitude 15.5° N; Longitude 44.2° E; Altitude 2199 m]. It seems temperatures in Sana'a are consistently higher than at Dhamar, but they follow the same pattern.

The meteorological station of Sana'a is located at a lower altitude, resulting in higher temperatures than in Dhamar. Compared to the coastal study areas, the temperature in the highlands is more variable, especially in the first four months of 2010. There is more day-to-day variation than in Hodeidah and Aden.

5.3 Fieldwork

In Dhamar a large part of the fields is classified in the field as furrow-irrigated. Locally fields are irrigated by border irrigation or by sprinklers. Most fields are used for two crops per year, although there are some fields that are rain fed and only accommodate one crop per year. Only some fields are used to produce qat in Dhamar.

6. Rada

6.1 General

Of the four study areas, Rada is the second highland area, just east of Dhamar, which is the other highland area.

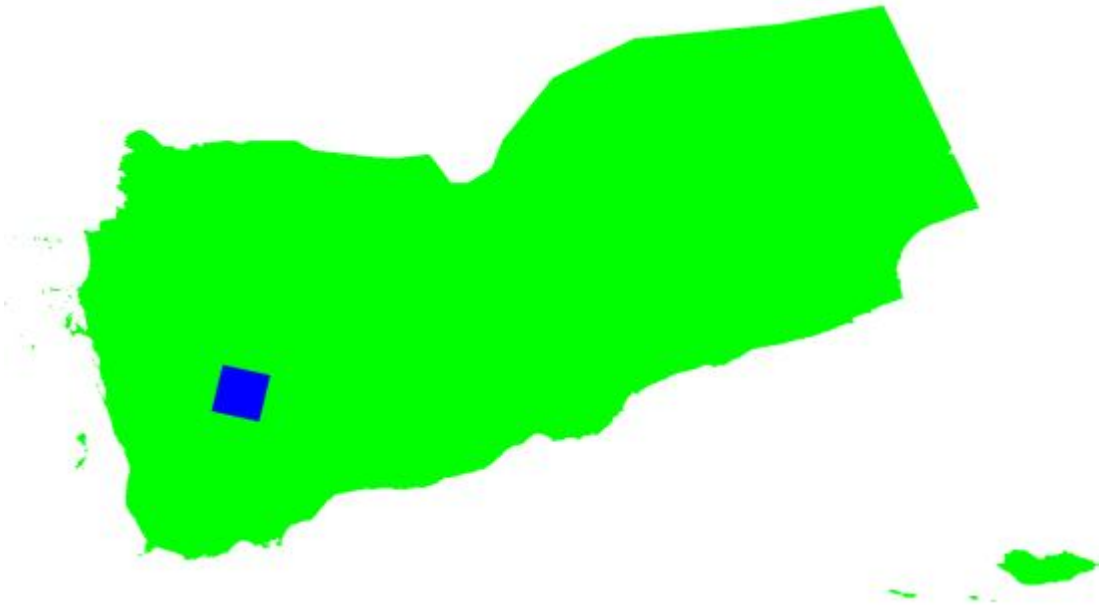

Figure 15: The Area of Interest of the Rada study area.

Like the Dhamar study area, Rada is located in the highlands of Yemen. The study area covers a part of Wadi Adhanah, which drains towards the desert area; and a part of Wadi Bana, draining towards the Gulf of Aden.

For Rada eleven satellite images are available: 3 images from Alos; 2 from Aster and 6 from Landsat. These 11 dates are well spread over the year.
The images made by Alos are shown on the next page. The images are displayed in so-called False Colour composite. This means that instead of displaying the bands blue, green and red (which would result in normal colours), the bands green, red and near-infrared are displayed. High measurements in the near-infrared part of the spectrum are shown as bright red in the images; these red areas mainly contain growing plants. In this way ‘bright red’ implies that the plants have water. In the image of July the red areas are brighter than in April. Next to the red areas, many parts of these images are grayish, indicating none or scarce vegetation in the mountains. In the image of 27 May 2010 also some clouds can be seen, they present themselves as white spots with black spots to the left of them. The clouds themselves reflect a lot of sunlight while casting a shadow on the land surface below, decreasing the reflection from the land under the shadow.

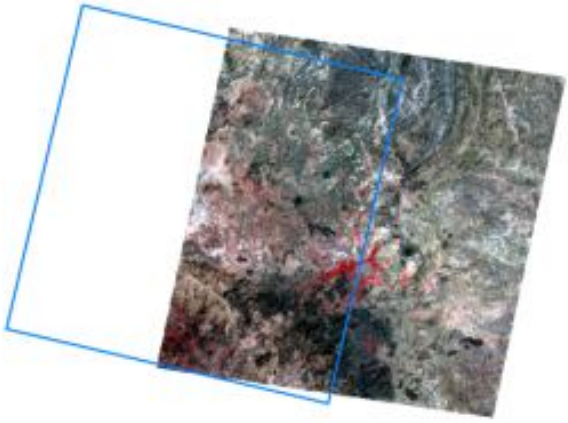

a) Aster - 22 October 2009

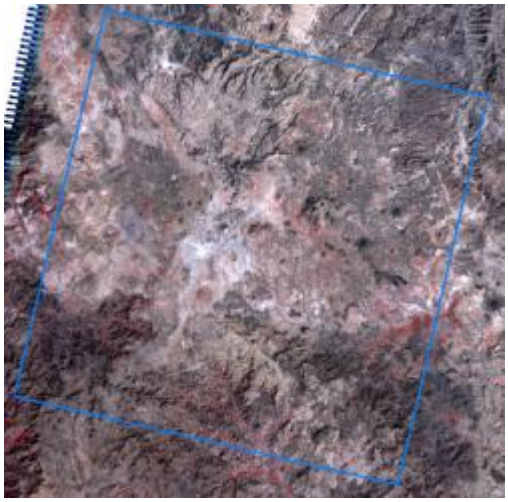

b) Landsat 5 - 18 January 2010

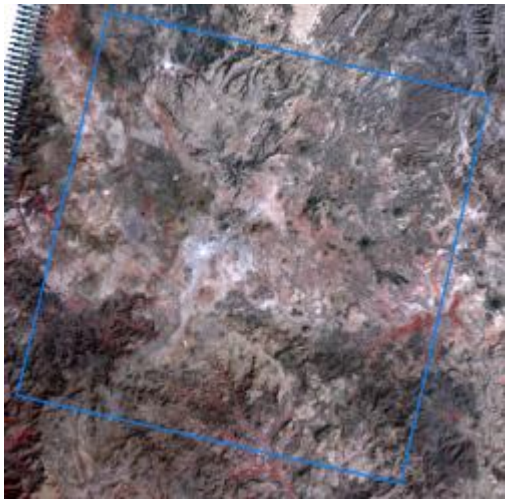

c) Landsat 7 - 26 January 2010

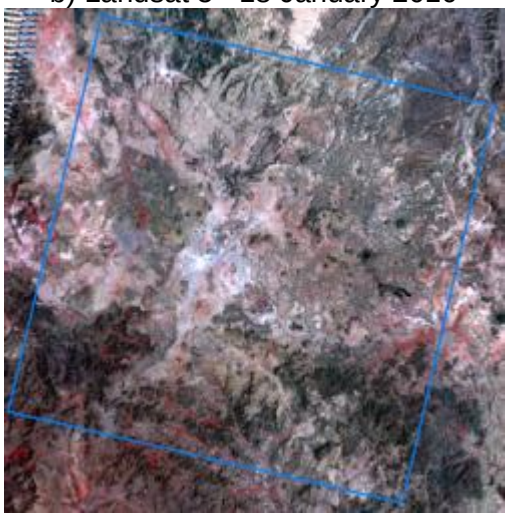

d) Landsat 7 - 15 March 2010

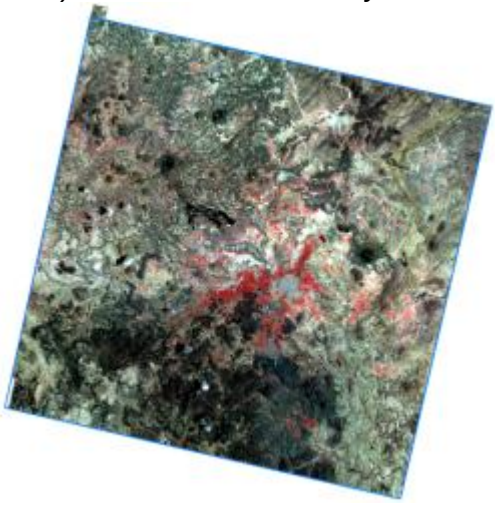

e) Alos - 11 April 2010

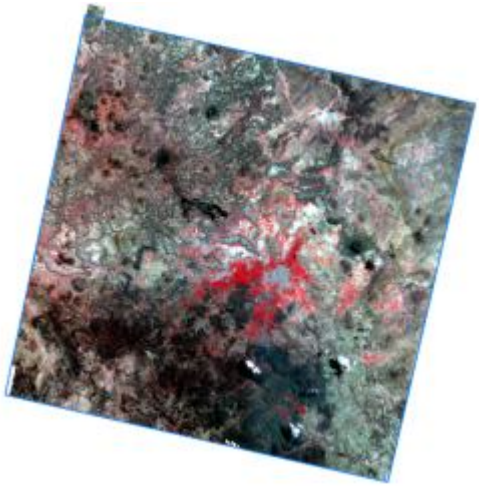

f) Alos - 27 May 2010

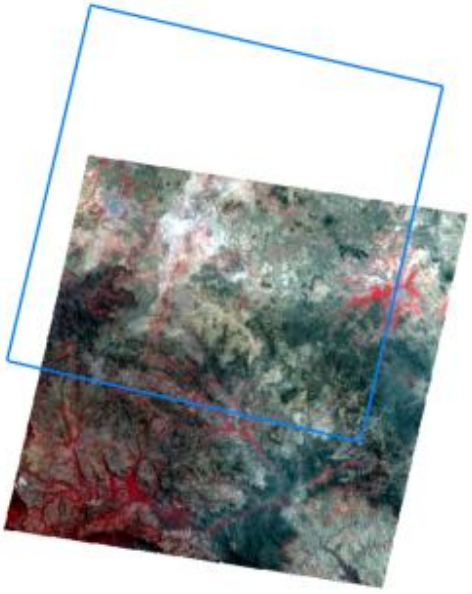

g) Aster - 26 June 2010

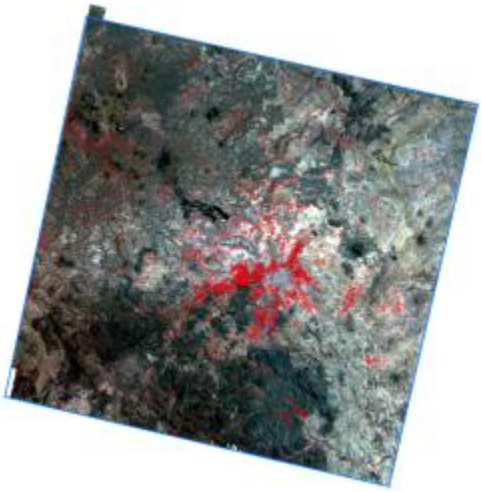

h) Alos - 12 July 2010

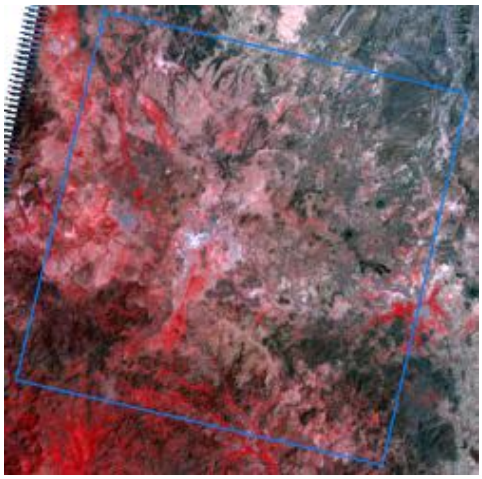

i) Landsat 7 - 23 September 2010

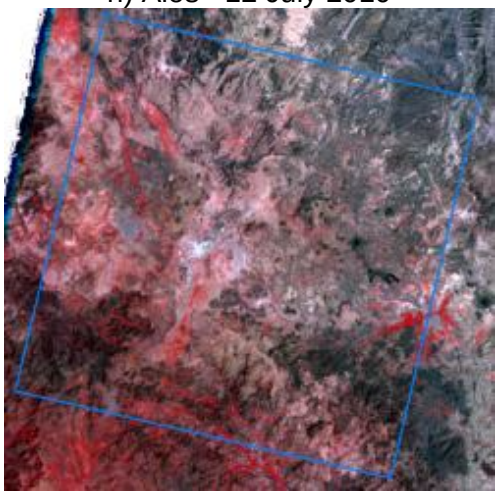

j) Landsat 7 - 09 October 2010

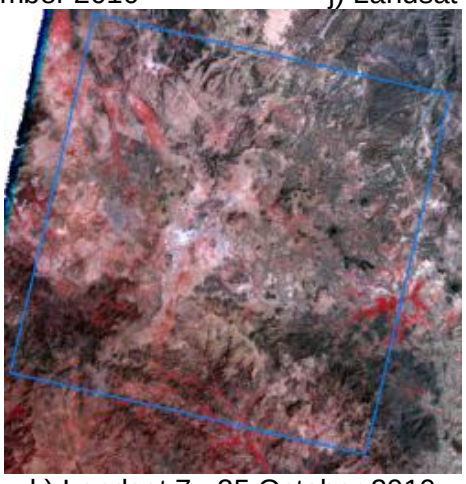

k) Landsat 7 - 25 October 2010

Figure 16: Satellite images for the study area Rada, with in blue the extent of the study area.

6.2 Climate

Figure 17 shows the total monthly precipitation for the Rada area in 2010, based on TRMM rainfall data. The rainfall pattern is very similar to that of Dhamar, caused by the overlap in area. The south-west of the study area receives slightly more rainfall than the north-eastern part of the study area. The average annual rainfall for 2010 is estimated to be 386 mm for Rada. For 2006 the amount of rain is estimated to be 437 mm. The difference between both years is that in 2006 there was a weak rainfall season in February, March, April, May, while in 2010 this first rainfall season yielded more rain. However, the second rainfall period in July, August, September gave less rain, causing a lower total sum over the year.

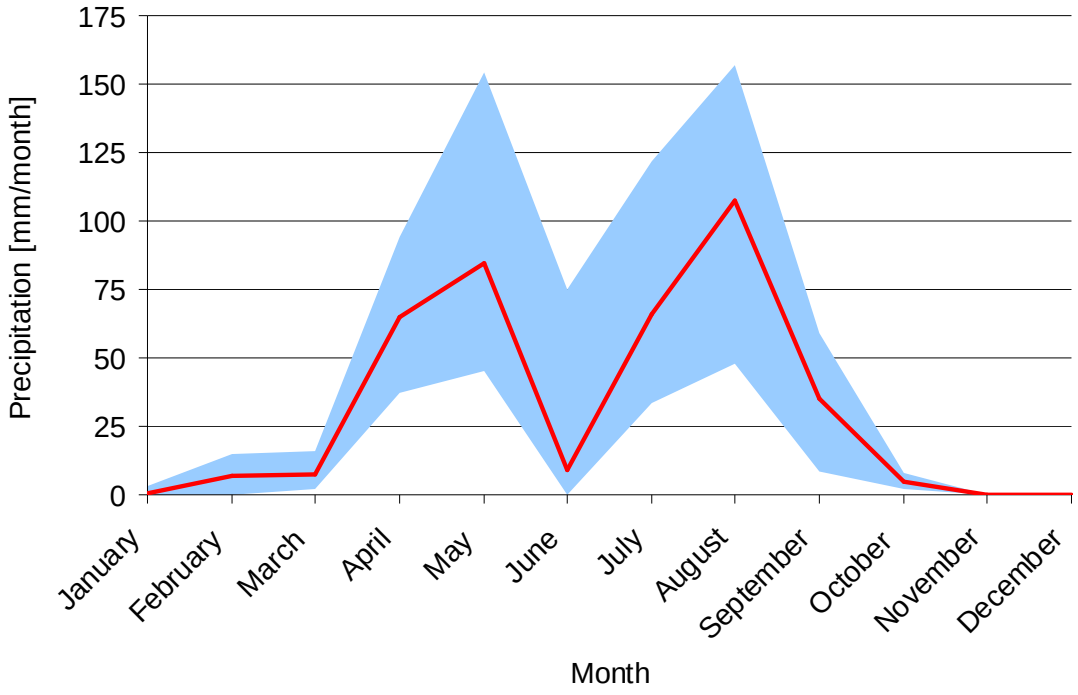

Figure 17: Monthly precipitation for the Rada area. The red solid line shows the average rainfall for the total area. The blue area shows the range of rainfall for the total area.

Figure 18: Location of the meteorological stations Sana'a (upper blue dot) and Dhamar (lower blue dot), with a blue outline of the Rada study area.

Since there are no measurements from meteorological stations in the Rada study area available, the same temperature measurements as for Dhamar are used to describe the climate in Rada. The location of these meteorological stations is shown in Figure 18. Figure 19 shows the air temperature as measured at the meteorological stations at Dhamar and Sana'a in 2010. There is an annual pattern in these measurements with temperatures in summer being approximately 10°C higher than in winter but with somewhat larger deviations from that pattern than for the coastal study areas.

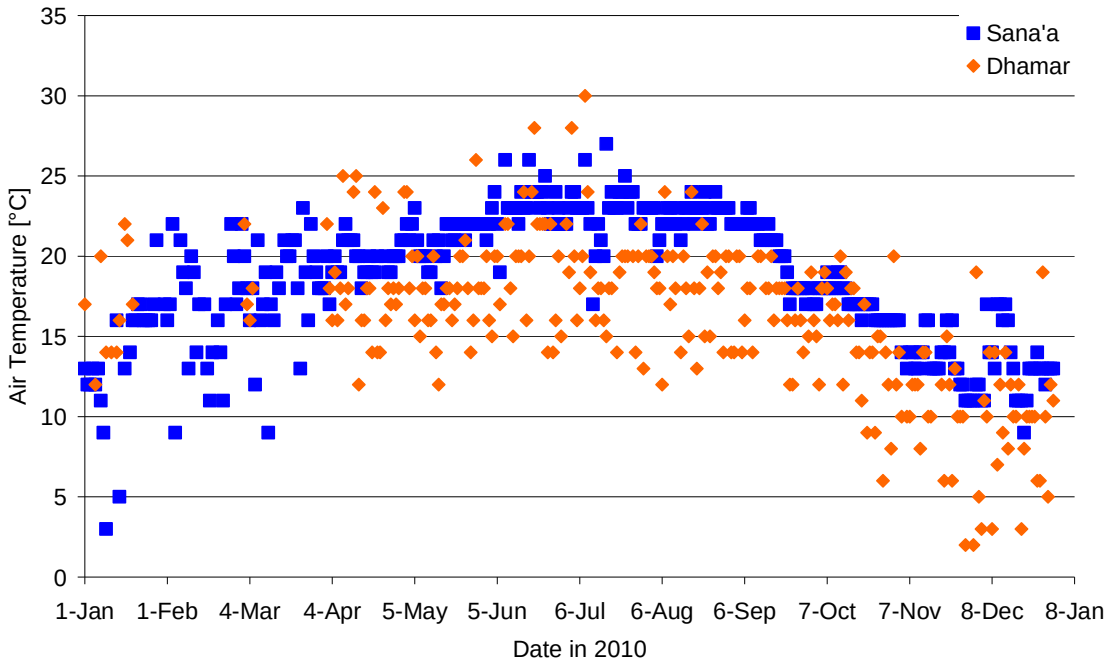

Figure 19: Daily air temperature values [°C] for the year 2010, Dhamar meteorological station [Latitude 14.6° N; Longitude 44.4° E; Altitude 2425 m]. In February and March periods are missing. Therefore also measurements from Sana'a meteorological station are shown [Latitude 15.5° N; Longitude 44.2° E; Altitude 2199 m]. It seems temperatures in Sana'a are consistently higher than at Dhamar, but they follow the same pattern.

The meteorological station in Dhamar is closest to the study area Rada. The temperatures measured at Dhamar indicate that the winter season might be too cold for agriculture, especially at higher altitudes.

6.3 Fieldwork

The vast majority of fields in the study area Rada is classified in the field inspection as producing qat. The remainder of fields is rain fed, single-season irrigated or double-season irrigated and the irrigation method in those fields is predominantly border irrigation.

7. Abyan

7.1 General

Of the four study areas, Abyan is the southern area, a delta at the coast of the Gulf of Aden.

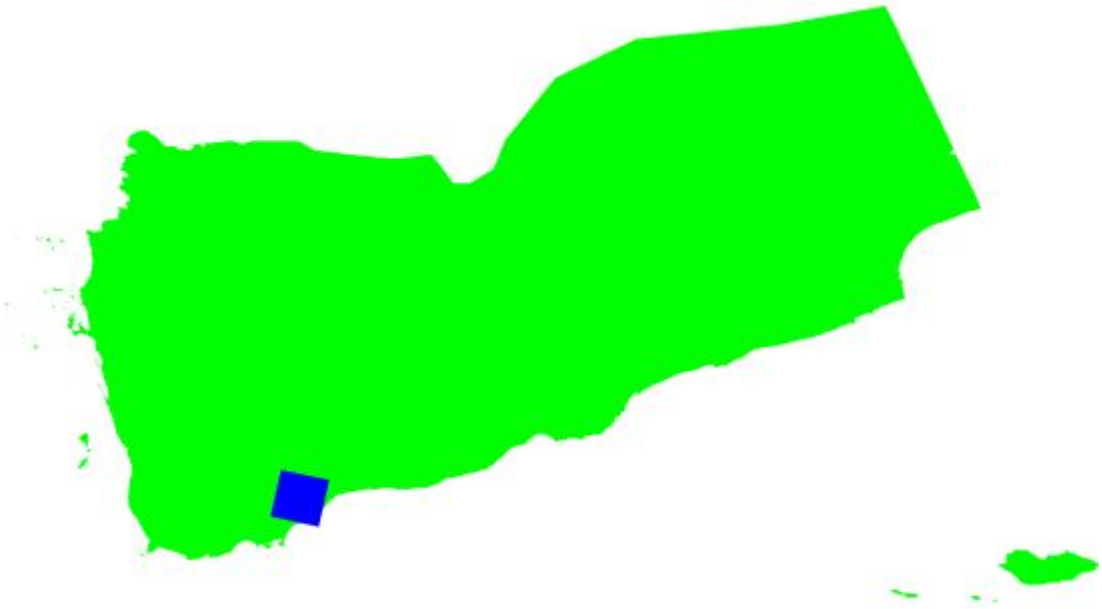

Figure 20: The Area of Interest of the Abyan study area.

Like the Siham study area, Abyan is a study area with wadis. The three major wadis in the study area are called Wadi Suhaybiyah, Wadi Bana and Wadi Hassan.

For Abyan less satellite images are available: 2 images from Alos; none from Aster and 6 from Landsat. These 8 dates are spread over the year but there is just one image in the period from April until September. The images made by Alos are shown on the next page. The images are displayed in so-called False Colour composite. This means that instead of displaying the bands blue, green and red (which would result in normal colours), the bands green, red and near-infrared are displayed. High measurements in the near-infrared part of the spectrum are shown as bright red in the images; these red areas mainly contain growing plants. In this way ‘bright red’ implies that the plants have water, for the dry season it means that the fields are irrigated. The main system of irrigation in the Abyan study area is spate irrigation, with most spates coming from runoff in Wadi Bana and a smaller fraction from Wadi Hassan. The irrigation water is distributed by a system of canals. But also groundwater is used as a source of irrigation water, especially for the fruit plantations in both the upper and the lower end of the Delta. The clearest difference between the two images shown here is the amount of growing vegetation in the centre of the image, in the upper end of the Delta; that area has more red spots in June than in March.

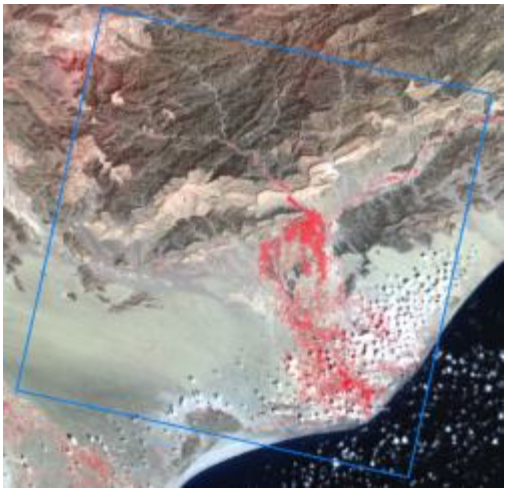

a) Landsat 7 - 22 October 2009

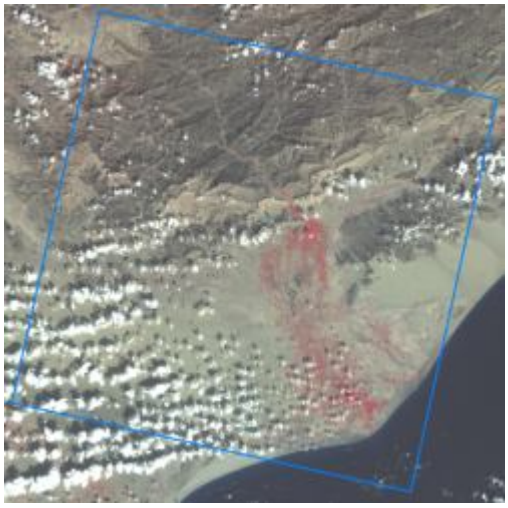

b) Landsat 5 - 17 December 2009

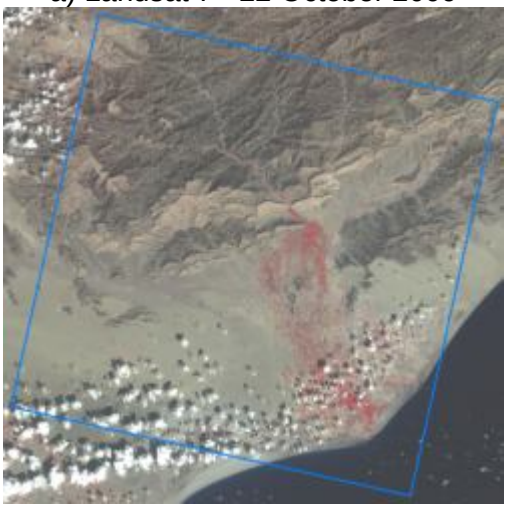

c) Landsat 5 - 18 January 2010

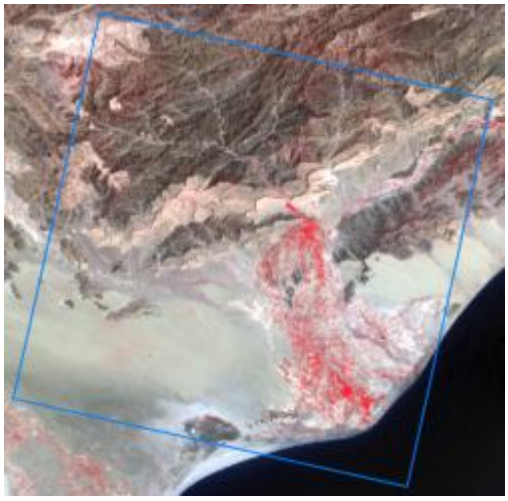

d) Landsat 7 15 March 2010

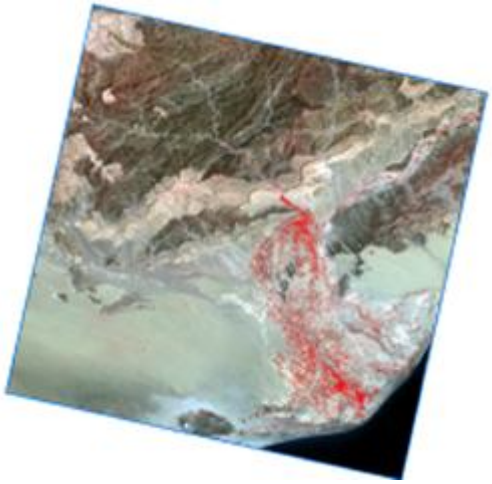

e) Alos - 25 March 2010

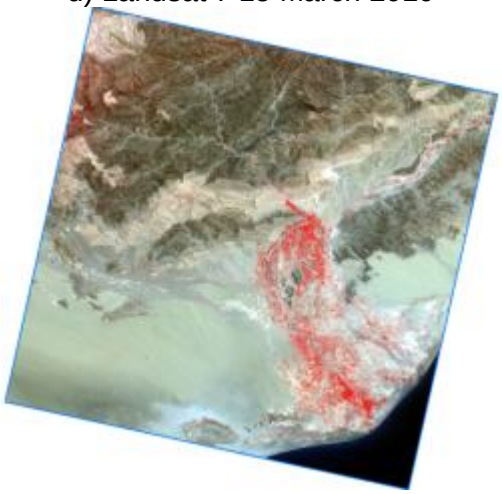

f) Alos - 25 June 2010

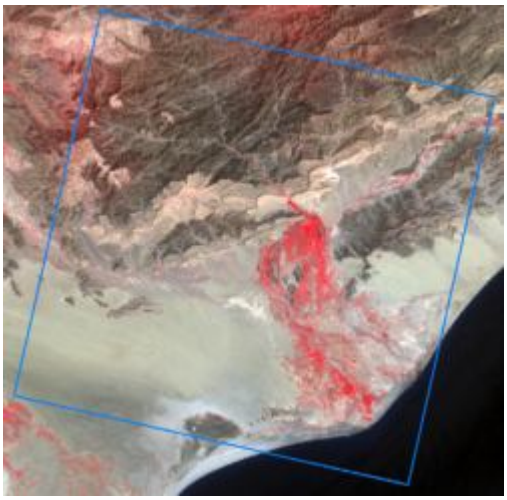

g) Landsat 7 - 09 October 2010

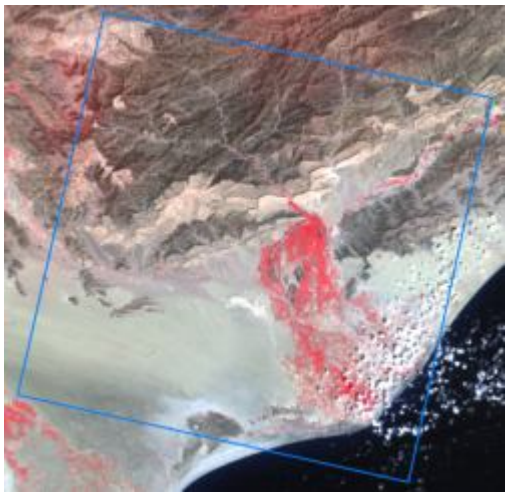

h) Landsat 7 - 25 October 2010

Figure 21: Satellite images of the Abyan study area, with in blue the extent of the study area.

7.2 Climate

Figure 7 shows the total monthly precipitation for the Abyan area in 2010, based on TRMM rainfall data. The coastal area in the south of the study area receives almost no rainfall. The average annual rainfall for 2010 is estimated to be 159 mm for Abyan, making Abyan the driest study area. For 2006 the amount of rain is estimated to be 201 mm. The lower amount of rain in 2010 is mainly due to less precipitation in July and August, which is only partly compensated by more precipitation in April and May.

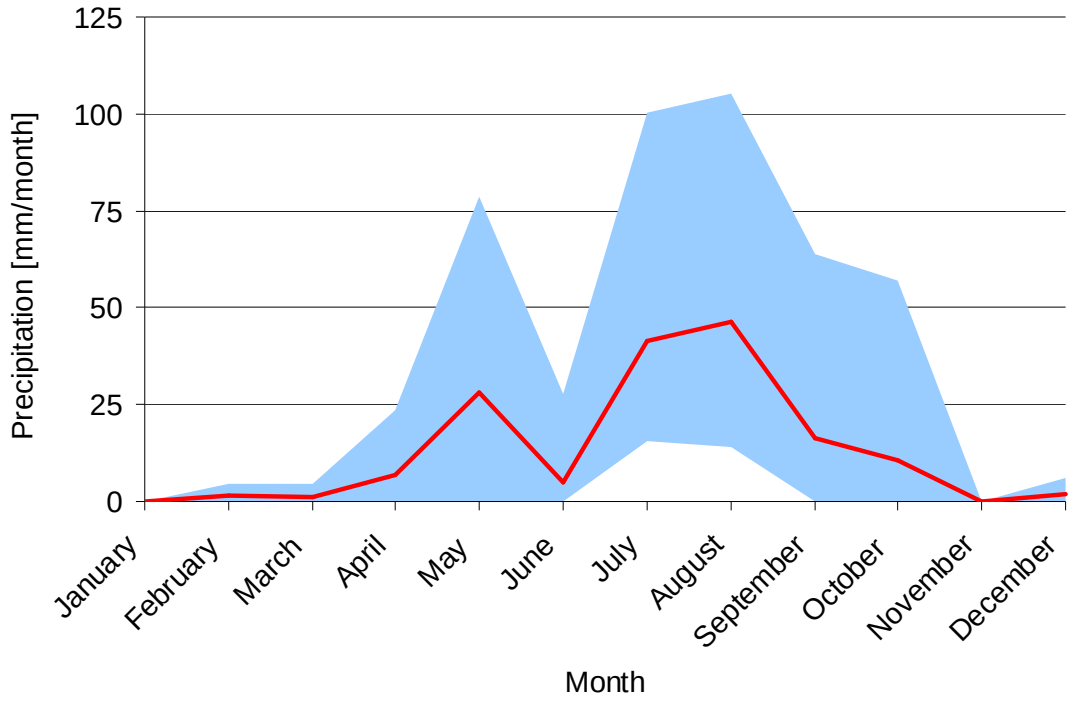

Figure 22: Monthly precipitation for the Abyan area. The red solid line shows the average rainfall for the total area. The blue area shows the range of rainfall for the total area.

To describe the climate, not only precipitation is an important factor, but also temperature. Temperature was measured at the meteorological station in Aden. The location of that station compared to the study area is shown in Figure 23. As can be seen in that figure, Aden is located outside the study area.

Figure 23: Location of meteorological station Aden (blue dot in the lower left corner) with a blue outline of study area Abyan.

Figure 23 shows the air temperature as measured at the meteorological station at Aden in 2010. There is an annual pattern in these measurements with temperatures in summer being approximately 10°C higher than in winter and with only small deviations from that pattern. It appears, however, that there is a small dip in temperatures in summer.

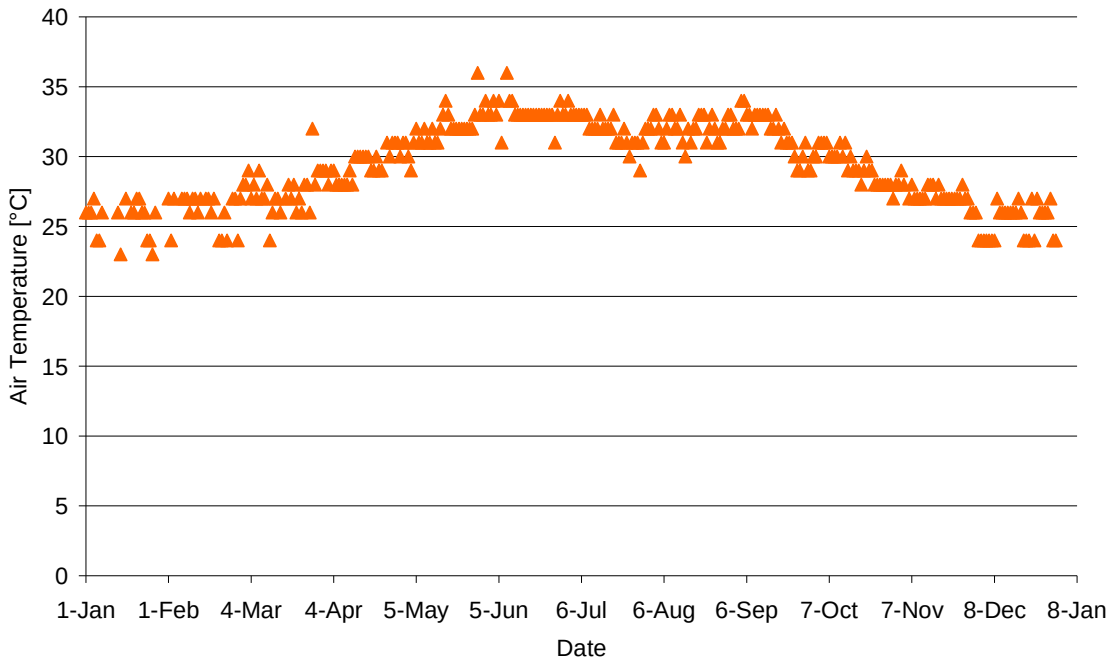

Figure 24: Daily air temperature values [°C] for the year 2010, Aden meteorological station [Latitude 12.8° N; Longitude 45.0° E; Altitude 3 m].

The meteorological station Aden, together with the station in Al Hudaydah, in the Siham study area, are the warmer locations with temperatures approaching 35°C, most probably due to their lower altitude: the meteorological station of Aden is located at an altitude of only 3 meters. Because of these high temperatures, crops will need more water, but the higher winter temperatures also accommodate a second cropping season, under the condition that there is sufficient water available.

7.3 Fieldwork

Due to the social instability in the Abyan study area, it has not been possible to conduct fieldwork.

8. Water balance analysis

On a catchment scale, precipitation is the most important incoming term of the water balance, ideally it would even be the only incoming term. An important outward term is evapotranspiration, the loss of water to the atmosphere. These two main terms can be combined to give the rainfall deficit. To calculate this, a simple calculation is done: rainfall – evapotranspiration. If the evapotranspiration exceeds the rainfall, other terms of the water balance will be affected: groundwater levels will drop and river flows will decrease.

For multiple catchments, average annual rainfall (paragraph 8.1) and evapotranspiration (paragraph 8.2) are calculated. The name and location of the catchments is shown in Figure 25.

Figure 25: Location of the wadis used in this study. Names are given for most, but not all, catchments.

8.1 TRMM Rainfall

The rainfall is estimated by measurements of the TRMM satellite. Due to a lack of ground based rainfall measurements the TRMM data could not be calibrated but it still provides a reasonable estimate and an idea of the spatial variation (Almazroui, 2010). The rainfall is accumulated for the year 2010 and averaged per catchment. The result is presented in Figure 26. Note that differences between coastal plains and highland areas within a catchment are averaged out. Because of this, the rainfall as shown for Wadi Bana, in which most of study area Abyan is located, is estimated to be between 300 and 400 mm/year, while the study area itself only received 159 mm of rain in 2010.

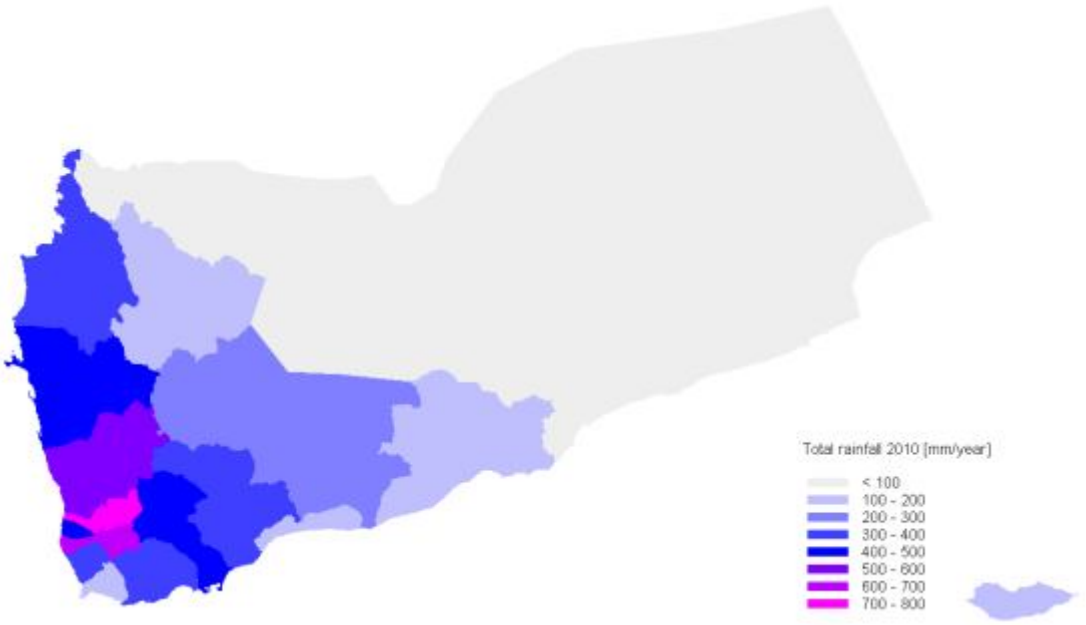

Figure 26: Total rainfall for 2010, averaged per catchment.

The rainfall trends are shown in Table 9. For the period of 1998 – 2010 the annual rainfall was calculated and of these 12 annual sums the average, minimum and maximum are shown. The column Trend represents the slope of the trend line of the 12 years, so the predicted rainfall for 2011 if the trend would be linear. The absolute trend alone does not reflect the impact, so also relative trend is calculated. Combining both absolute and relative trend reflects the change better. For example: although the absolute trend in Wadi Zabid seems strong, it is only a small relative change. On the other hand: while the absolute trend in Maifaah Catchment is much smaller, compared to the total amount of rain, it's much stronger.

Table 9: Rainfall trends in fourteen wadis in Yemen from 1998 to 2010.

Catchment	Average [mm/year]	Minimum [mm/year]	Maximum [mm/year]	Trend [mm/year]	Relative trend [%]
Wadi Adhanah	200	67	304	-6.8	-3%
Wadi Surdud	313	225	492	7.1	2%
Wadi Siham	392	235	560	-3.8	-1%
Hajar Catchment	135	37	282	8.6	6%
Ramlat as Sabatayn	144	37	223	-1.6	-1%
Wadi Rima'	431	237	563	-5.8	-1%
Maifaah Catchment	84	27	166	4.8	6%
Wadi Zabid	656	327	839	-14.1	-2%
Wadi Bana	291	112	494	-0.3	0%
Wadi Ahwar	145	45	233	3.0	2%
Wadi Nakhlah	486	336	894	-7.2	-1%
Wadi Tuban	416	229	611	-1.1	0%
Wadi Rasyan	809	507	974	-3.5	0%
Wadi Mawza'	536	435	692	4.1	1%

In Figure 27 and Figure 28 the annual rainfall of the same period as Table 9 is plotted to see the pattern in time. The catchments are split up in a group of seven catchments at the Gulf of Aden or inland and a group of seven wadis at the coast of the Red Sea. From these graphs it is clear that 2009 was a dry year for all catchments. The total amount of precipitation in 2010 is closer to the average, but in most catchments lower than in 2006.

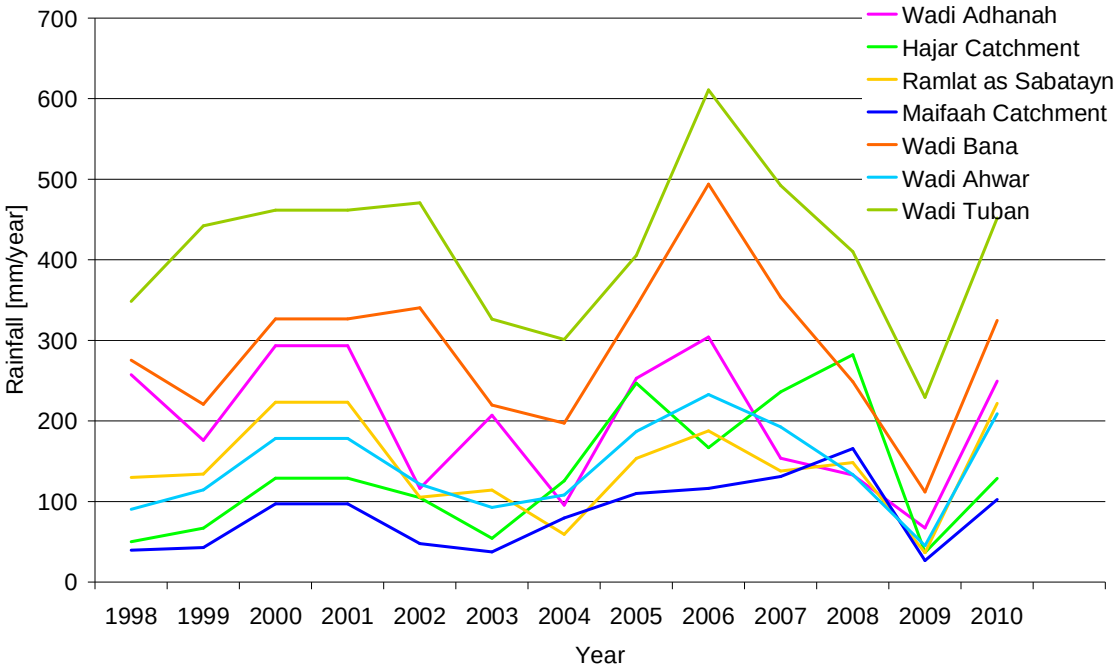

Figure 27: Rainfall trends from 1998 to 2010 for the catchments at the Gulf of Aden and land inwards.

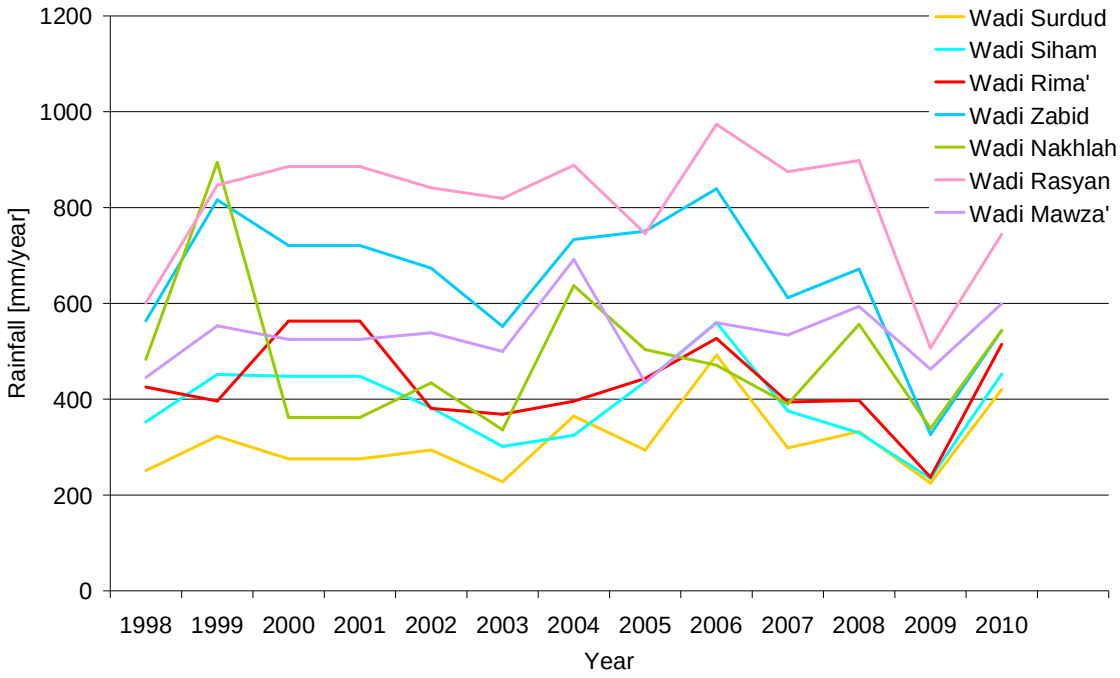

Figure 28: Rainfall trends from 1998 to 2010 for the wadis at the Red Sea coast.

Literature

Almazroui, M., 2010. Calibration of TRMM rainfall climatology over Saudi Arabia during 1998-2009. *Atmospheric Research* 99, 400-414.

WaterWatch, Hydro-Yemen, Euroconsult Mott McDonald, 2009. Satellite Imagery for Cropping Pattern and Irrigated Area Monitoring. Performed under assignment of the Ministry of Agriculture and Irrigation of Republic of Yemen and financed by the World Bank.

Appendix 1 SEBAL description

Algorithm overview

The Surface Energy Balance Algorithm for Land (SEBAL) is an image-processing tool comprised of 25 computational steps that calculates the actual (ET_{act}) and potential evapotranspiration rates (ET_{pot}) as well as other energy exchanges between land and atmosphere. The key input data for SEBAL consists of spectral radiance in the visible, near-infrared and thermal infrared part of the spectrum (see Figure 29). SEBAL computes a complete radiation and energy balance along with the resistances for momentum, heat and water vapour transport for every individual pixel. The resistances are a function of state conditions such as soil water potential (and thus soil moisture), wind speed and air temperature and change from day-to-day.
Satellite radiances will be converted first into land surface characteristics such as surface albedo, leaf area index, vegetation index and surface temperature. Additional input used in deriving the land surface characteristics consists of a digital elevation model (DEM) and a land use map. The land used map should discriminate between water, vegetated areas, bare soil and built-up area. The land surface characteristics can be derived from different types of satellites.

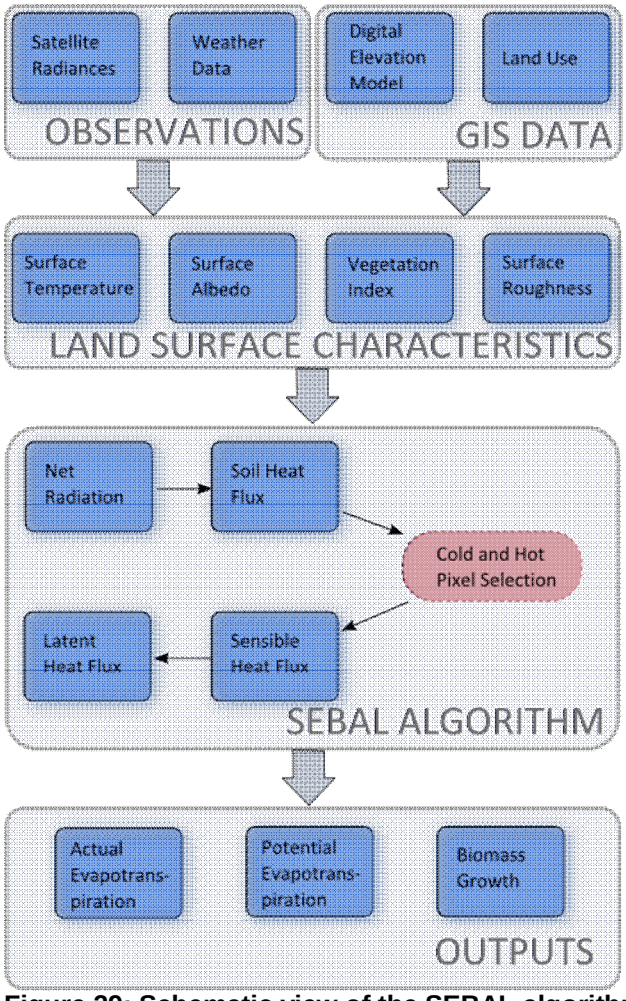

Figure 29: Schematic view of the SEBAL algorithm.

Data requirements

In addition to satellite images, the SEBAL tool requires the following routine weather data parameters:

- Wind speed
- Humidity
- Solar radiation
- Air Temperature

There is limited data on land use needed, and no data on soil type or hydrological conditions is required to apply SEBAL.

SEBAL Evapotranspiration

The primary basis for the SEBAL tool is the surface energy balance. The instantaneous ET_{act} flux is calculated for each cell of the remote sensing image as a 'residual' of the surface energy budget equation:

$$ET = R_n - G - H \qquad [W/m^2] \qquad (1)$$

Where; ET is the latent heat flux [W/m^2], R_n is the net radiation flux at the surface [W/m^2], G is the soil heat flux [W/m^2], and H is the sensible heat flux to the air [W/m^2], see Figure 30. The terms of the surface energy balance are different for different type of surfaces. For vegetation the ET value is larger than the H flux. For bare soil the situation is vice versa. SEBAL uses these differences in energy balance behaviour for the different surfaces to get a first estimate on the surface energy balance for all pixels.

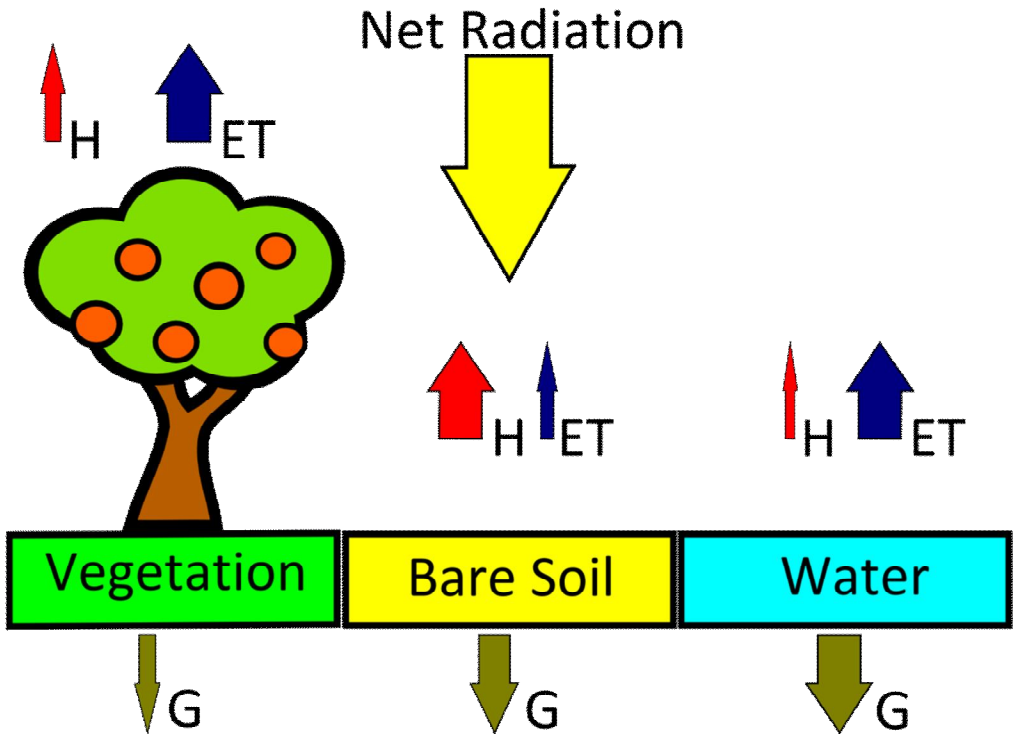

Figure 30: Surface Energy Balance for different types of surfaces

R_n represents the actual radiant energy available at the surface. It is computed by subtracting all outgoing radiant fluxes from all incoming radiant fluxes. This is further specified in the surface radiation balance equation:

$$R_n = R_{S\downarrow} - \alpha R_{S\downarrow} + R_{L\downarrow} - R_{L\uparrow} - (1 - \varepsilon_0) R_{L\downarrow} \quad [W/m^2] \qquad (2)$$

where $R_{S\downarrow}$ is the incoming short-wave radiation [W/m^2], α is the surface albedo (dimensionless), $R_{L\downarrow}$ is the incoming long wave radiation [W/m^2], $R_{L\uparrow}$ is the outgoing long wave radiation [W/m^2], and ε_o is the surface thermal emissivity (dimensionless).

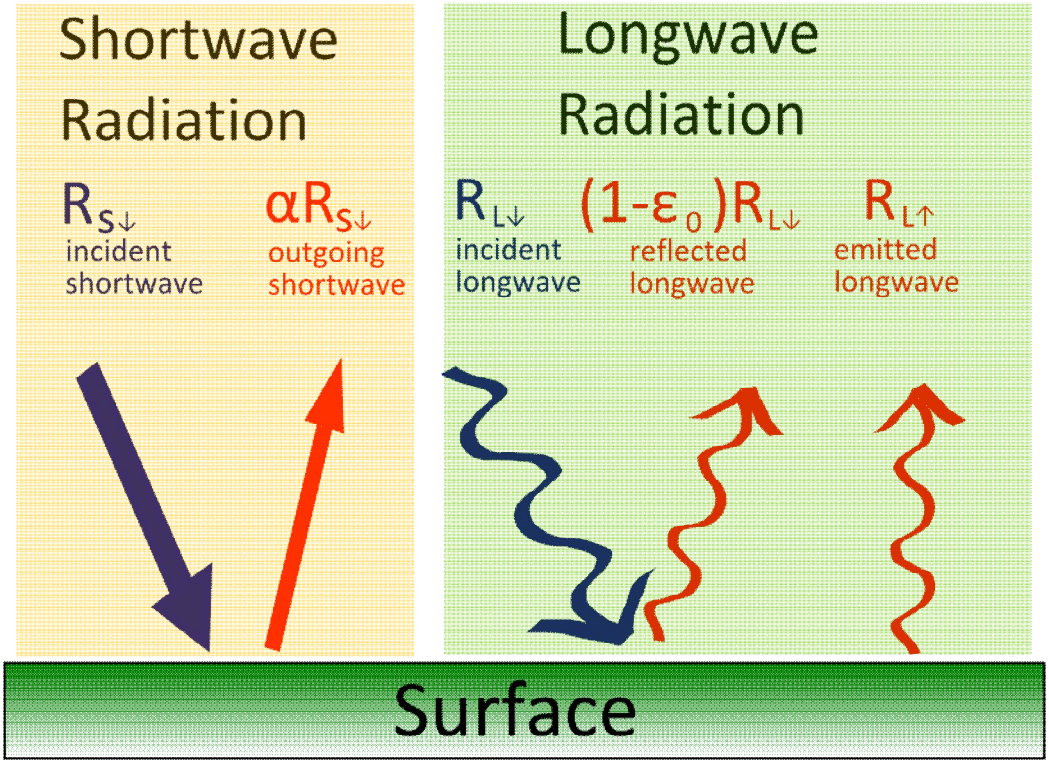

Figure 31: Surface Radiation Balance

In Equation (2), the amount of net short-wave radiation ($R_{S\downarrow}$ - αR_S) that remains available at the surface, is a function of the surface albedo (α). The broad band surface albedo α is derived from the narrow band spectral reflectance's α(λ) measured by each satellite band. The incoming short-wave radiation (R_S) is computed using the solar constant, the solar incidence angle, a relative earth-sun distance, and a computed broad band atmospheric transmissivity. This latter transmissivity can be estimated from sunshine duration or inferred from pyranometer measurements (if available). The incoming long wave radiation (R_L) is computed using a modified Stefan-Boltzmann equation with an apparent emissivity that is coupled to the shortwave atmospheric transmissivity and a measured air temperature. Outgoing long wave radiation (R_L) is computed using the Stefan-Boltzmann equation with a calculated surface emissivity and surface temperature. Surface temperatures are computed from the satellite measurements of thermal radiances.

In Equation (1), the soil heat flux (G) and sensible heat flux (H) are subtracted from the net radiation flux at the surface (R_n) to compute the "residual" energy available for evapotranspiration (λE). Soil heat flux is empirically calculated as a G/R_n fraction using vegetation indices, surface temperature, and surface albedo. Sensible heat flux is computed using wind speed observations, estimated surface roughness, and surface to air temperature differences that are obtained through a sophisticated self-calibration between dry (λE≈0) and wet (H≈0) pixels. SEBAL uses an iterative process to correct for atmospheric instability caused by buoyancy effects of surface heating.
The λE time integration in SEBAL is split into two steps. The first step is to convert the instantaneous latent heat flux (λE) into daily λE24 values by holding the evaporative fraction constant. The evaporative fraction EF is:

$$EF = \lambda E / (R_n - G) \qquad [-] \qquad (3)$$

Field measurements under various environmental circumstances have indicated that EF behaves temporally stable during the diurnal cycle. Since EF ~ EF24, i.e. the 24 hour latent heat flux can be determined as:

$$\lambda E24 = EF\ R_{n,24} \qquad [W/m^2] \qquad (4)$$

For simplicity, the 24 hour value of G is ignored in Equation (4). The second step is the conversion from a daily latent heat flux into monthly values, which has been achieved by application of the Penman-Monteith equation:

$$\lambda E_{PM} = (sa\ R_{n,24} + \rho_a c_p\ \Delta e/ra) / (s_a + \gamma\ (1 + r_s/r_a)) \qquad [W/m^2] \qquad (5)$$

where s_a (mbar/K) is the slope of the saturated vapor pressure curve, $\rho_a c_p$ (J/m3 K) is the air heat capacity, Δe (mbar) is the vapor pressure deficit, γ (mbar/K) is the psychrometric constant and ra (s/m) is the aerodynamic resistance. The parameters s_a, Δe and r_a are controlled by meteorological conditions, and R_n and r_s by the hydrological conditions.
The SEBAL computations can only be executed for cloudless days. The result of λE24 from Eq. (4) has been explored to convert the Penman-Monteith equation (Eq. 5) and to quantity r_s inversely using $\lambda E_{24} = \lambda E_{PM}$. The spatial distribution of r_s so achieved, will consequently be used to compute λE_{24} by means of Equation (5) for all days without satellite image available (Bastiaanssen and Bandara, 2001). The total ET_{act} for a given period can be derived from the longer term average λE flux by correcting for the latent heat of vaporization and the density of water.